Copernicus Marine Service

QUALITY INFORMATION DOCUMENT

WAVE Thematic Assembly Centre:

WAVE_GLO_PHY_ SWH_L3_NRT _014_001

cmems_obs-wave_glo_phy-swh_nrt_s6a-l3_PT1S

dataset-wav-alti-l3-swh-rt-global-j3

dataset-wav-alti-l3-swh-rt-global-s3a

dataset-wav-alti-l3-swh-rt-global-s3b

dataset-wav-alti-l3-swh-rt-global-al

dataset-wav-alti-l3-swh-rt-global-c2

dataset-wav-alti-l3-swh-rt-global-cfo

dataset-wav-alti-l3-swh-rt-global-h2b

dataset-wav-alti-l3-swh-rt-global-h2c

dataset-wav-alti-l3-swh-rt-global-swon

Issue: 3.4

Contributors: N. Taburet, R. Husson, E. Charles, G. Jettou, A. Philip, S. Philipps, M. Ghantous, C. Kocha

Approval date by the CMS product quality coordination team: 12/12/2023

CHANGE RECORD

When the quality of the products changes, the QuID is updated, and a row is added to this table. The third column specifies which Sections or Sub-sections have been updated. The fourth column should mention the version of the product to which the change applies.

Issue	Date	§	Description of Change	Author	Validated By
1.0	February 2018	All	First version of document at CMEMS V4, done from previous SeaLevel-TAC QUID for the wave component	R Husson, N Taburet, E Charles	Mercator Océan
1.1	June 2018		Accounts for the integration of the new L3 SWH dataset for Cryosat-2	N Taburet, E Charles	Mercator Océan
2.0	January 2019	All	Evolution of L3 products and integration of Sentinel-3B mission	N Taburet	
3.0	September 2019	All	Evolution of L3 products with EMD filtering Addition of a new field Integration of CFOSAT mission	N. Taburet	Mercator Ocean
3.1	May 2020	All	Integration of HaiYang-2B mission Addition of altimetry-derived wind field	G. Jettou, E. Charles	E. Charles
3.2	March 2022	All	Integration of Sentinel-6A mission	E. Charles, A. Philip	E. Charles
3.3	September 2022	All	Update of the absolute calibration Integration of HaiYang-2C mission Change of product names	A. Philip, S. Philipps, M. Ghantous, C. Kocha	R. Husson
3.4	October 2023	All	Integration of SWOT nadir mission	A. Philip	P. Zunino

TABLE OF CONTENTS

I EXECUTIVE SUMMARY

I.1 Products covered by this document

This document describes the quality of the operational (Near Real Time - NRT) along-track significant wave height (SWH) products listed hereafter:

Product	WAVE_GLO_PHY_SWH_L3_NRT_ 014_001
Area	Global ocean
Missions	Sentinel-6A; Jason-3; Sentinel-3A; Sentinel-3B; SARAL/AltiKa; Cryosat2; CFOSAT ; HaiYang-2B ; HaiYang-2C, SWOT nadir
Spatial resolution	Along-track ~7 km (full 1 Hz resolution)
Temporal resolution	Variable with satellite cycle length: 10 days for Sentinel-6A and Jason-3, 27 days for Sentinel-3A and Sentinel-3B, drifting orbit (non-cyclic) for SARAL/AltiKa and Cryosat2, 13 days for CFOSAT, 14 days for HaiYang-2B, 10 days for HaiYang-2C, 28 days for SWOT nadir . Products are stored in 3-hour length files, updated every hour.

The number of altimeter data processed by the system varies with time, according to satellite availability and version updates. Table 1 summarizes the periods during which the datasets for each mission are available for the current version. The latest version includes the 10-m wind speed derived from altimeters and therefore starts only from the beginning of year 2020.

Note: Previous versions (with a different file format) cover a longer historical period and are available on request to the WAVE TAC production centre (through the Copernicus Marine Environment Monitoring Service (**CMEMS) service desk).**

	Temporal availability	
	Begin date	**End date**
S3A	01/01/2020	Present
S3B	01/01/2020	Present
J3	01/01/2020	Present
AL	01/01/2020	Present
C2	01/01/2020	Present
CFO	01/01/2020	Present
H2B	07/07/2020	Present
S6A	17/12/2020	Present
H2C	29/11/2022	Present
SWOT nadir	29/11/2023	Present

Table 1: Temporal period processed by the L3 alti wave chain for the different datasets. Those periods are necessarily shorter than L2 availability presented in Table 5. This product is available at present date with a few hours delayed.

I.2 Summary of the results

The quality of the along-track significant wave height (SWH) product is controlled at each step of the L3 alti wave processing chain. This chain evolved in April 2019 in order to use L2P wave products as input and to apply a Lanczos low-pass filter to reduce the along-track noise. Since December 2019 (product version 3.0), the filtering method has evolved and now uses a method based on Empirical Mode Decomposition (EMD), following Quilfen and Chapron [2019]. Since July 2020, this product now includes a 10-m wind field derived from altimeter measurements and collocated to the significant wave height measurements.

Upstream L2P products are processed in an independent processing chain. This chain takes L2 products in input and performs the editing, the cross-calibration and the absolute calibration with respect to buoys. Details of these processes in the L2P wave chain are in section VII as they are of great importance for the L3 wave product quality.

Table 2 and Table 3 present the mean bias and standard deviation at crossover between the different missions and Jason-3 at the L2P level (calibration) and L3 level (filtering).

As expected, the calibration step mainly reduces the inter-mission bias. The filtering process also improves it, but its contribution is mainly to reduce the standard deviation of the crossover differences.

Cross-compared missions	Before cross-calibration		After cross-calibration (performed in L2P chain)	
	Bias [cm]	Standard dev. [cm]	Bias [cm]	Standard dev. [cm]
Sentinel-3A / Jason-3 (1)	8.2	26.7	-1.1	25.4
Sentinel-3B / Jason-3 (1)	7.4	26.2	-2.0	25.0
SARAL-AltiKa / Jason-3 (1)	5.9	22.7	0.7	22.7
Cryosat2 / Jason-3 (1)	0.9	24.3	0.3	24.4
CFOSAT / Jason-3 (1)	-8	35	TBC	TBC
HaiYang-2B / Jason-3 (2)	15.5	24	-0.3	23
Sentinel-6A / Jason-3 (tandem) (3)	-0.7	3	-0.5	2
HaiYang-2C / Sentinel-6A	TBC	TBC	TBC	TBC
SWOT nadir / Jason-3	1.4	11.3	0.33	11.3

Table 2: Bias and standard deviation between Jason-3 and secondary missions' SWH, before and after the calibration step (L2P processing chain). Computation period: (1) February 17th 2019 to July 31st 2019; (2) March 9th 2021 to March 9th 2022; (3) December 1st 2021 to February 15th 2022 (tandem). Period used for SWOT is August 1st 2023 to September 12th2023.

Cross-compared missions	After cross-calibration (performed in L2P chain)		After Filtering (performed in L3 chain)	
	Bias [cm]	Standard dev. [cm]	Bias [cm]	Standard dev. [cm]
Sentinel-3A / Jason-3	-1.1	25.4	-1.0	21.3
Sentinel-3B / Jason-3	-2.0	25.0	-1.6	21.2
SARAL-AltiKa / Jason-3	0.7	22.7	0.5	18.8
Cryosat2 / Jason-3	0.3	24.4	0.4	19.6
CFOSAT / Jason-3	TBC	TBC	TBC	TBC
HaiYang-2B / Jason-3	-0.3	23	-0.3	19.5
Sentinel-6A / Jason-3 (tandem)	-0.5	2	-0.5	2
HaiYang-2C / Sentinel-6A	TBC	TBC	TBC	TBC
SWOT nadir / Jason-3	0.33	11.3	0.33	11.3

Table 3: Bias and standard deviation between Jason-3 and secondary missions' SWH, before and after the filtering step (L3 processing chain). Computation period: see Table 1.

I.3 Estimated Accuracy Numbers

The noise measurement error (i.e., uncorrelated error) of the VAVH_UNFILTERED field (before along track filtering) is given in Table 4. The average noise is the uncertainty associated with the 1-Hz significant wave height estimates. It is the standard deviation of the high frequency (HF) measurements used to compute the 1 Hz value, divided by the square root of the number of HF points. The AltiKa mission's lower noise level is because of its higher-frequency sampling (40 Hz compared to 20 Hz for the other missions).
The along track filtering should reduce these uncertainties in most areas.

Mission	Average noise (cm rms)
Jason-3	12
Sentinel-3A & B (SAR mode)	9
SARAL/AltiKa	6
Cryosat2	9
CFOSAT	9
HaiYang-2B	4.5
Sentinel-6A	9
HaiYang-2C	3
SWOT nadir	12

Table 4: Mean 1 Hz noise measurement observed for the different altimeters before denoising (VAVH_UNFILTERED). Unit: cm rms.

Uncertainties were also estimated with a cross-over validation (two satellite measurements are compared at cross-over locations). Results are shown in Table 3.

II PRODUCTION SYSTEM DESCRIPTION

II.1 Production centre name

WAVE-CLS-TOULOUSE-FR

II.2 Operational system name

The operational chain is given a generic name: the L3 alti wave chain.

II.3 Main principles of the altimeter-derived Significant Wave Height (SWH) and wind speed measurements

The altimeter sends a spherical radar signal in the direction of the nadir (top part of Figure 1). This signal is reflected by the sea surface and goes back to the satellite. The analysis of the returned signal allows the calculation of the time needed by the signal to go and come back, i.e. the distance satellite-sea surface. The sea state surface elevation distribution (middle part of Figure 1) impacts the speed at which the return signal is fully returned to the satellite. Hence, the Significant Wave Height (SWH) over ocean surfaces is determined from the slope of the front in the radar altimeter wave form (bottom part of Figure 1). The higher the waves, the more the returned signal is spread in time. In other word, the slope of the radar altimeter wave form is lower for higher waves. Hence, a long delay between the first returns and a full signal return will result in a long shadow in the wave form, which then indicates a high sea state (Figure 1 and Figure 2). For more technical details see https://www.aviso.altimetry.fr/en/techniques/altimetry/principle/pulses-and-waveforms.html.

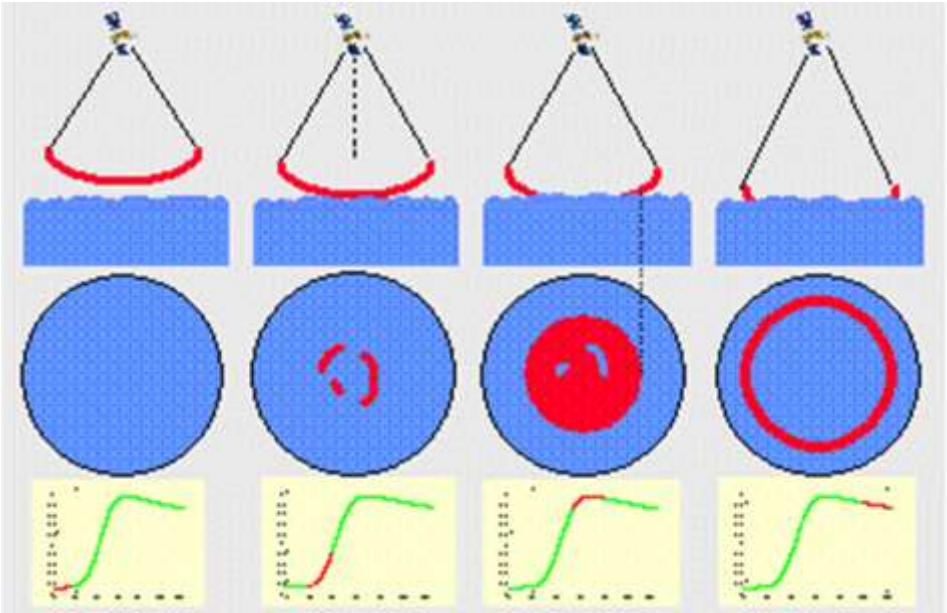

Figure 1: Formation of an echo over a sea surface with waves for conventional altimetry.

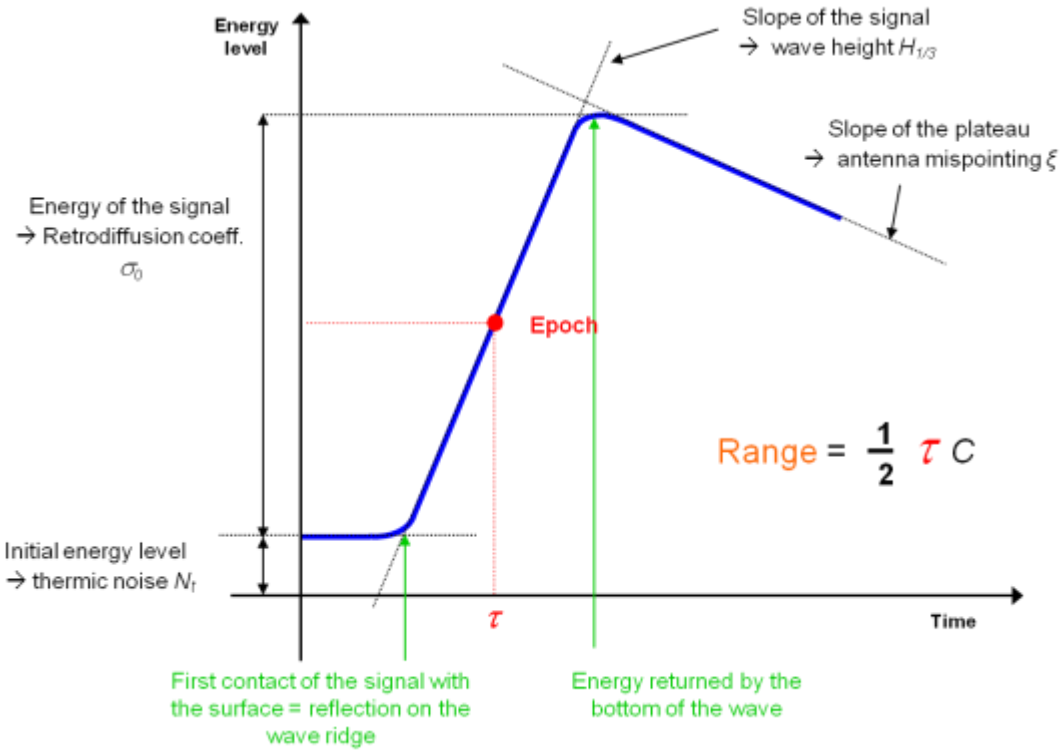

Figure 2: The altimeter waveform.

The term Significant Wave Height (SWH or H_s) refers to the mean wave height of the highest third of the waves (also sometimes denoted $H_{1/3}$) (slope of the signal in Figure 2). The backscatter coefficient which is the amplitude of the altimetry waveform (σ_0 in Figure 2) can be related to wind speed. Wind across the surface of the ocean affects is roughness, which in turn affects the backscatter of the radar altimetry pulse. A stronger wind speed results in a smaller backscatter, and a lower sigma0 value. Different algorithms were developed to propose a relation between the wind speed, and the sea surface backscatter coefficient and eventually the significant wave height. The wind speed model function is usually evaluated for 10 metres above the sea surface.

II.4 Production centre description for the version covered by this document

The system's primary objective is to provide operational products of calibrated significant wave height (SWH) and collocated wind speed data for operational altimeter missions. The L3 processing sequence can be divided into 3 main steps, illustrated in Figure 3 and described in the next Sub-sections:

- Acquisition
- Filtering
- Product generation.

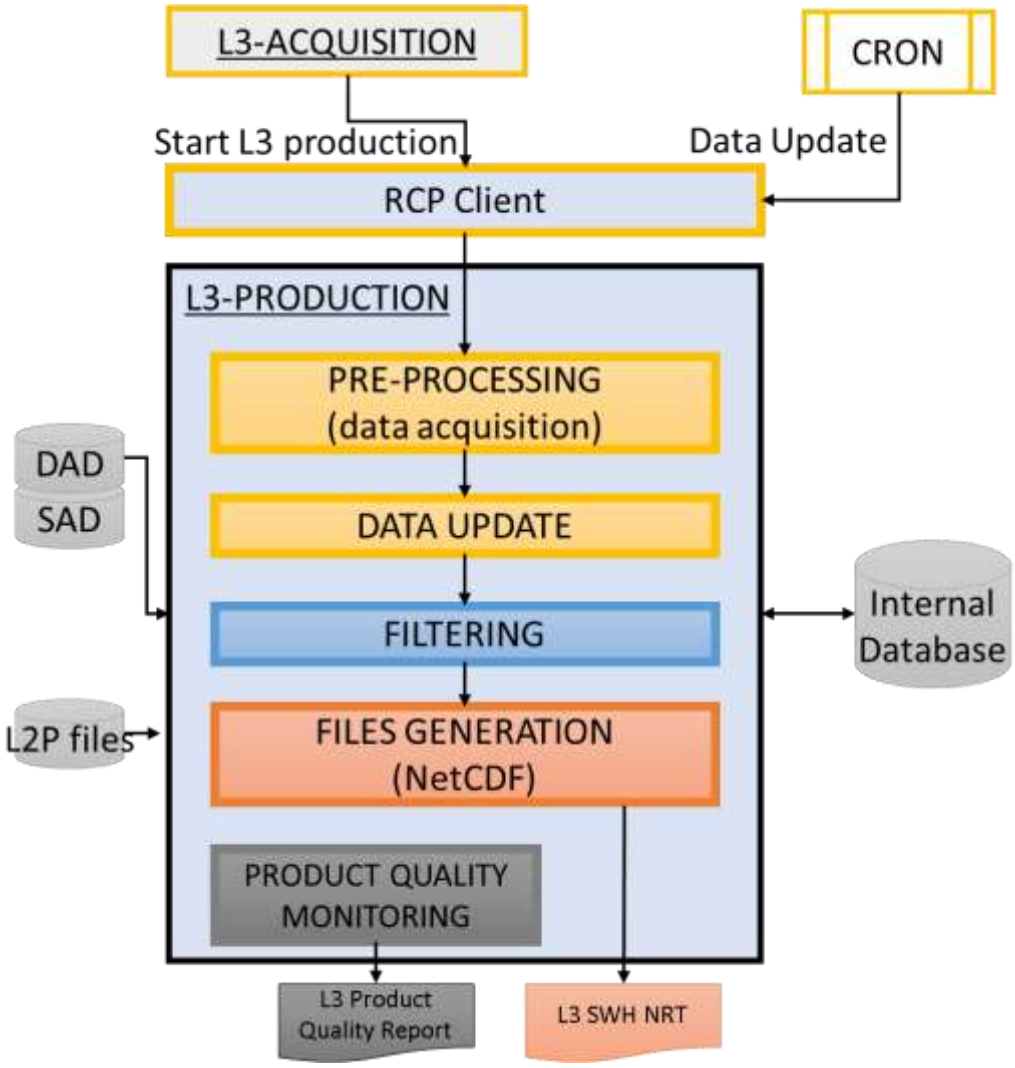

Figure 3: L3 Alti wave production component. Where RCP is Remote Call Procedure, DAD is Dynamic Acquired Data, SAD is Static Acquired Data, SWH is Significant Wave Height and NRT is Near Real Time.

II.4.1 Acquisition

The altimeter measurements used in the system consist of Near-Real-Time Level 2P products from different missions. These L2P products are along-track products, produced within 1 hour of the L2 availability from the different agencies. The source, delay and period of availability of both L2 and L2P products are summarised in Table 5 and Table 6. Regarding Cryosat2, L2 NRT Ocean Product (NOP) data are available from 2011, however, the enhanced L2 version processed with baseline C chain is available only from January 22nd, 2018. Mission characteristics are presented in Table 7. We point out that the L2 availability period is longer than that of the L3-wave products which were added to the L3 WAVE-TAC system later (see Table 1). For the CFOSAT mission, only the nadir altimetry SWH measurements are used in the L3 SWH wave products.

Mission	Type of product	Source	Availability delay	Period of availability
Jason-3	OGDR	EUMETSAT/NOAA	~3 h	2016/12/13 (cycle 12) – present
Sentinel-3A	NRT	ESA/EUMETSAT	~3 h	2016/02/17 (cycle 1) – present
Sentinel-3B	NRT	ESA/EUMETSAT	~3 h	2018/06/06 (cycle 9) – present
SARAL/AltiKa	OGDR	EUMETSAT	~3 h	2013/03/14 (cycle 1) – present
Cryosat2	NOP	ESA	~3 h	2011/01/01 (cycle 13) – present
CFOSAT	NRT	CNES	~3 h	2019/04/25 – present
HaiYang-2B	IGDR	CNES/NSOAS	~48 hours	2019/11/15 – present
Sentinel-6A	OGDR	ESA/EUMETSAT	~3 hours	2020/17/12 - present
HaiYang-2C	IGDR	CNES/NSOAS	~48 hours	29/11/02 - present
SWOT nadir	OGDR	CNES/JPL	~3 hours	01/08/23 - present

Table 5: Source, delay and period of availability of the different L2 altimeter data (delay is relative to measurement time).

Mission	Type of product	Source	Availability delay
Jason-3	L2P NRT	Non-disseminated products	~1 h
Sentinel-3A	L2P NRT	EUMETSAT	~1 h
Sentinel-3B	L2P NRT	EUMETSAT	~1 h
SARAL/AltiKa	L2P NRT	Non-disseminated products	~1 h
Cryosat2	L2P NRT	Non-disseminated products	~1 h
CFOSAT	L2P NRT	CNES	~1 h*
HaiYang-2B	L2P STC	Non-disseminated products	~1 h
Sentinel-6A	L2P NRT	EUMETSAT	~1 h
HaiYang-2C	L2P STC	Non-disseminated products	~1h
SWOT nadir	L2P NRT	CNES/JPL	~1 h

*Table 6: Source and delay of availability of the different L2P altimeter data (delay is relative to L2 availability). *CFOSAT being an exploratory mission, the upstream L2P operational production has more relaxed constraints than for the other missions.*

Mission	Cycle duration (days)	Latitude range (°N/S)	Number of tracks per cycle	Inter-track distance at equator (km)	Sun-synchronous	Technology
Jason-3	10	±66	254	~315	No	LRM
Sentinel-3A	27	±81.5	770	~104	Yes	SAR + PLRM
Sentinel-3B	27	±81.5	770	~104	Yes	SAR + PLRM
SARAL/AltiKa	Non-cyclic (since July 2016)	±81.5	1002 (per pseudo cycle)	~80	Yes	LRM
CryoSat-2	29 (sub cycle)	±88	840	~98	No	LRM + SAR + SARIN
CFOSAT	13	±83	394	TBC	Yes	LRM (nadir + off nadir)
HaiYang-2B	14	±81	386	~210	Yes	LRM
Sentinel-6A	10	±66	254	~315	No	LRM
HaiYang-2C	10	±66	274	293	Yes	LRM
SWOT nadir	28	±77.6	584	120	No	LRM

Table 7: Altimeter mission characteristics. Sentinel-3B's orbit is shifted from Sentinel-3A's to cover a complementary ground track pattern interleaved between two Sentinel-3A tracks. Since S6A is reference mission, Jason-3 shifted (on the 7/04/2022) from reference orbit to interleaved between to reference tracks. In the Technology column, SAR is Synthetic Aperture Radar, LRM is Low Resolution Mode and PLRM is Pseudo LRM.

Finally, Table 8 details the different wind algorithms available in the native Level-2 products and used in the Level-3 wave products. The acquired wind speed data are then intercalibrated with the reference mission Jason-3 (see VII.1.2.4). No noise filtering is applied to the wind measurements.

Mission	Wind algorithm	Type
Jason-3	Gourrion et al. [2002] & Collard [2005]	2-parameter (sigma0 and SWH)
Sentinel-3A	Gourrion et al. [2002] & Collard [2005]	2-parameter (sigma0 and SWH)
Sentinel-3B	Gourrion et al. [2002] & Collard [2005]	2-parameter (sigma0 and SWH)
SARAL/AltiKa	Tran [2014]	2-parameter (sigma0 and SWH)
CryoSat-2	Abdalla [2007]	1-parameter (sigma0)
CFOSAT	Not used	Not used
HaiYang-2B	NSOAS	NSOAS
Sentinel-6A	Gourrion et al. [2002] & Collard [2005]	2-parameter (sigma0 and SWH)
HaiYang-2C	NSOAS	NSOAS
SWOT nadir	Gourrion et al. [2002] & Collard [2005]	2-parameter (sigma0 and SWH)

Table 8: wind speed algorithms available in the native Level-2 products and used in the Level3 wave products.

The acquisition processing has two main functions: acquisition and synchronization of dataflow as illustrated in Figure 4.

File acquisition

The purpose of the acquisition is to acquire new L2P files and new ancillary data (AUX files) needed to compute the products (orbit file, external corrections, etc.) for each data source.

Each L2P file acquired can be updated with its availability date read on the source server. This ensures that the most recent input files are being used and avoids unnecessary updates.

Data synchronization

The synchronization function synchronizes L2P data with all ancillary data (AUX files) needed to process L3 data. Once the L2P data and all the associated ancillary data are available, they can be used for L3 production.

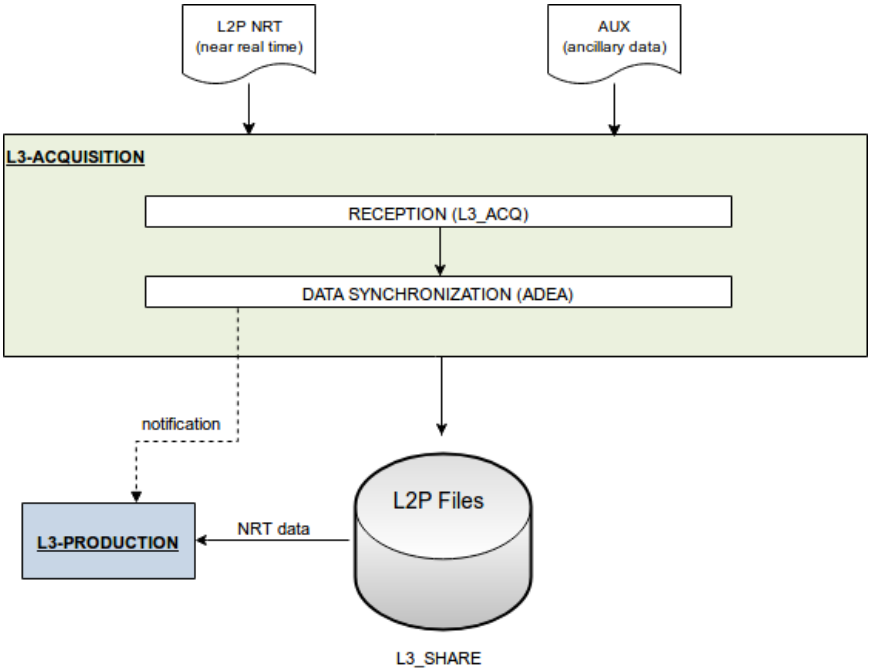

Figure 4: L2P acquisition processing.

II.4.2 Filtering process

A filtering algorithm has been applied to the acquired L2P product since v3.0 of the L3 alti wave chain. First based on a low-pass Lanczos filter, since v4.0 the filtering process has been based on Empirical Mode Decomposition (EMD).

EMD consists in decomposing the signal into so-called intrinsic mode functions (IMF). These functions are computed from the input signal by means of an iterative process (sifting); therefore, they are signal dependant, in contrast with standard decomposition methods (e.g. wavelets). This is particularly suited for signals, such as significant wave height, with a variable noise distribution and for which it is difficult to find suitable basis functions.

The implementation of the empirical mode decomposition and filtering follows the work of Kopsinis [2009] that has been fine tuned for SWH signal processing by Quilfen and Chapron [2019]. Although the EMD and Lanczos filter produce similar results in areas with weak small-scale dynamics (Figure 5, top), there is a more significant difference in areas of stronger small-scale dynamics (Figure 5, bottom) where the Lanczos filtering flattens the high gradient and peak values much more strongly. EMD does not suffer from this behaviour and allows denoising of the data without smoothing the small-scale information. This result was also reported by Quilfen and Chapron [2019].

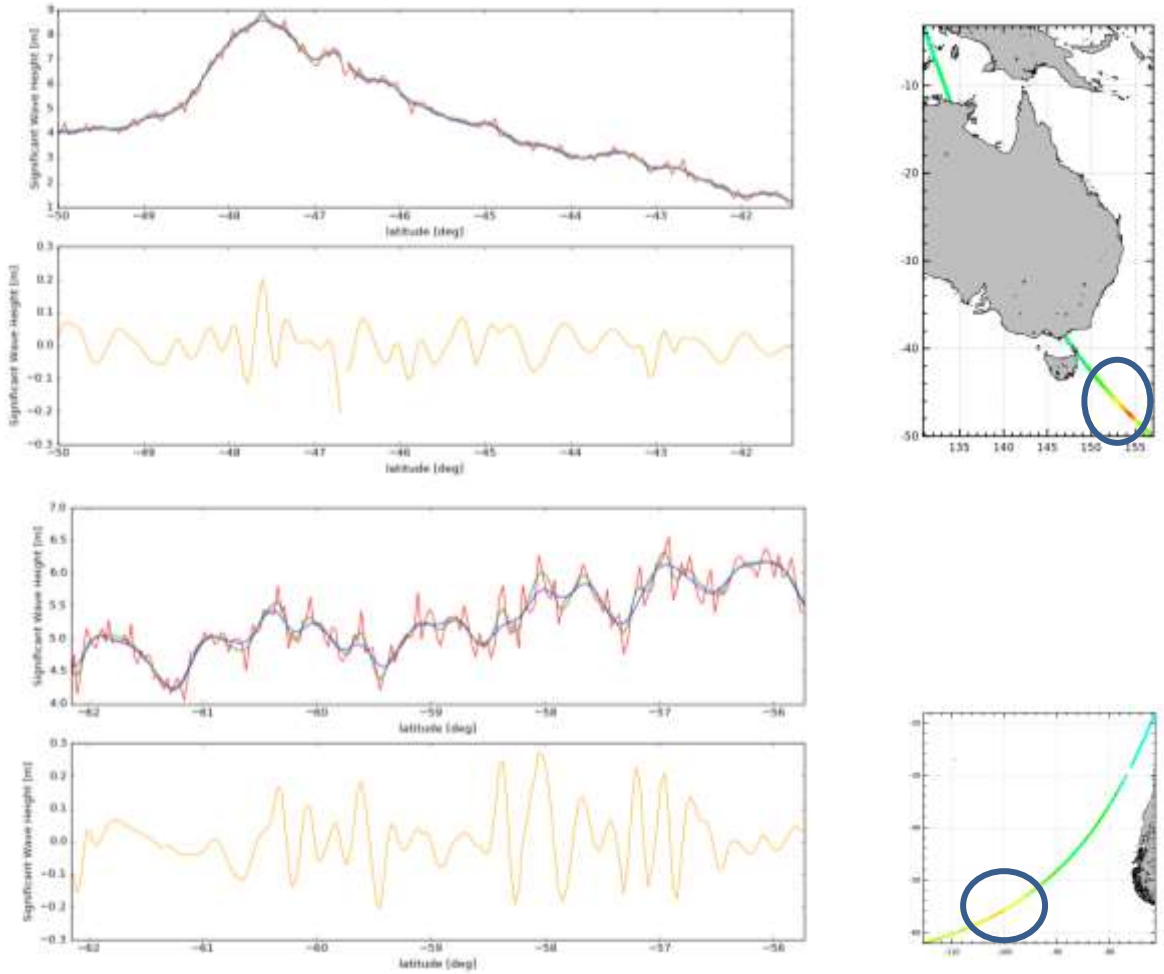

Figure 5: Comparisons between unfiltered SWH (L2P product, in red) and the L3 v3.0 with EMD filtering (green) and L3 v2.0 with Lanczos filtering (blue). The orange plot represents the difference between the SWH obtained with EMD and Lanczos filtering. Jason-3 data on 19th April 2019. The two upper plots on the left correspond to data recovered on a region of weak small-scale dynamics, region circled on the upper right plot. The two lower plots on the left correspond to data recovered on a region of strong small-scale dynamics, region circled on the lower right plot.

Figure 6 illustrates the power spectra computed between +/- 66° latitude for the period covering the 14th of February 2019 to the 2nd of August 2019. As shown by the dashed lines, the L2P measurements are contaminated by noise at scales lower than 100 km. The different noise levels at different frequencies can be characterised by the instrumental noise (at the highest frequencies) and the hump artefact [Dibarboure et al. 2014]. With the Lanczos filter, all fluctuations (signal as well as noise) at scales smaller than 60 km were removed, therefore suppressing the meso-scale signal of interest. This excessive smoothing is avoided with the EMD-based method as shown by the solid lines. The EMD method denoises the SWH down to scales of the order of 25 km, scales at which the signal to noise ratio is too low to recover the underlying signal as explained in Quilfen and Chapron [2019].

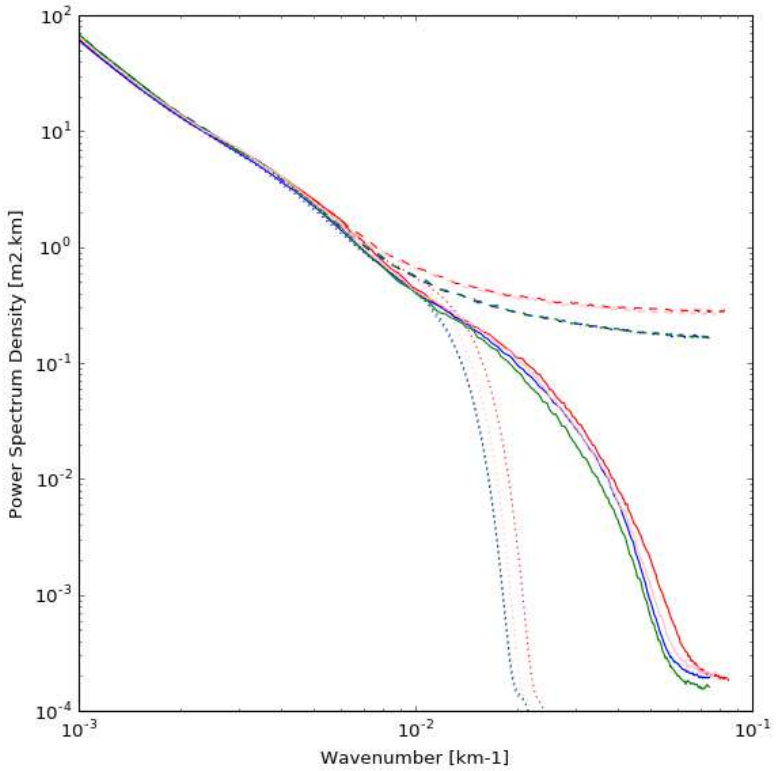

Figure 6: Power spectra of altimeter SWH measurements for Jason-3 (red), Sentinel-3A (blue), Sentinel-3B (green) and Cyosat2 (pink) over the period 14th February 2019 to 2nd August 2019. Dashed lines represent the power spectra of the L2P 1 Hz calibrated SWH data. The solid lines represent the power spectra of the L3 1 Hz data filtered with the EMD method. The dotted lines represent the power spectra of the former v2.0 L3 products obtained by Lanczos filtering with a 60 km cut-off scale.

This filtering is applied to valid L2P SWH values. These time series are divided into segments satisfying the following conditions:

- No gaps of more than two seconds
- No more than one consecutive flagged point
- Segments shorter than 8 points are not processed as they are too short for robust IMF decomposition and their filtered value is set to the default value.

The filtering method requires that each segment have a dyadic length (i.e., in the form 2^n with n being an integer). To that end, segments are set to such lengths before filtering by means of a symmetrical extension on the right and left. The segments are of course truncated back to their original size after processing and only the filtered values of available original data are kept.

II.4.3 Product generation and quality control

The filtering process described in the previous section is applied to valid L2P SWH values issued from all missions. One NetCDF file per 3-hour period is generated for each mission. The time ranges are 0 h-3 h, 3 h-6 h etc., in universal time. The processing and L3 product generation and update with the latest received data are triggered every 30 minutes. Since product version 1.1 the format was upgraded to NetCDF4.

The L3 along-track products contain the fields described in Table 9.

Name	**Standard name**	**Long name**	**NetCDF Type**	**Units**	**Comment**
time	time	time (sec. since 2000-01-01)	double	seconds since 2000-01-01 00:00:00.0	
latitude	latitude	latitude	int	10^{-6} deg	
longitude	longitude	longitude	int	10^{-6} deg	
VAVH	sea_surface_wave_ significant_height	significant wave height on main altimeter frequency band	short	10^{-3} m	Bias corrected and filtered
VAVH_UNFILTERED	sea_surface_wave_ significant_height	significant wave height on main altimeter frequency band	short	10^{-3} m	Bias corrected. Unfiltered
WIND_SPEED	wind_speed	Equivalent 10-m wind speed derived from altimeter measurements	short	10^{-3} m s^{-1}	Bias corrected

Table 9: Along-track significant wave height variables and dimensions included in each L3 NetCDF file.

Daily automated controls are performed, and upon generation, warnings are sent to operators.

Quality control reports are also generated once a day and regularly analysed by altimetry experts (internal validation, these reports are not disseminated). Sections III and IV.1 present the diagnostics implemented in these reports.

III VALIDATION FRAMEWORK

The validation evaluates the quality of the produced significant wave height and the performance of the key processing steps. Different aspects of both the L2P and L3 processing are assessed:

- The data availability and spatial and temporal coverage
- The data editing monitoring (L2P quality flag)
- The multi-mission cross-calibration monitoring (combination of the L2P calibration process and L3 filtering process)
- The ocean signal consistency.

Table 10 lists the different metrics that are used. They mainly consist of analyses of the SWH field at different steps of the processing and of checking the consistency of SWH along the tracks of different altimeters.

Uncertainties affecting the produced significant wave height can also be investigated through specific studies carried out at different steps of the processing. Their results are presented in Section IV.3.

Name	Description	Ocean parameter	Supporting reference dataset	Quantity
L3				
SWH_L2P-NC-AVAIL-<period>	Number of altimeter measurements missing/available	Significant Wave Height	None	Missing data are identified over the data flow processed Temporal evolution of the number of measurements on a daily/weekly/monthly basis and/or along each track of the altimeter considered. The current method is not suitable for drifting missions and is therefore not implemented for Saral/AltiKa. An update is planned to address this.
SWH_L2P-NC-VALID-<period>	Number of altimeter measurements valid/invalid	Significant Wave Height	None	Valid/rejected data are identified over the data flow processed Temporal evolution of the number of measurements on a daily/weekly/monthly basis and/or along each track of the altimeter considered.
SWH_L2P-NC-MEAN_T	SWH signal monitoring	Significant Wave Height	None	Temporal evolution of the weekly-averaged significant wave height estimated between +/- 66° latitude estimated over several months for each mission for all/valid data. The associated temporal evolution of the number of all/valid samples should also be attached for missions with high latitude sampling.
SWH_L2P-NC-ALT-MEAN_T-XOVER	SWH differences at mono- and multi-missions crossover positions	Significant Wave Height	None	Temporal evolution of the weekly-averaged mean difference between two SWH measurements corresponding to altimeter track crossover positions (typically estimated over several days). The performance of the product before and after calibration (inter-calibration, absolute calibration wrt. *in situ*) is compared.
POS_SWH_L2P-CLASS3-ALT-VALID-XOVER-<period>				Temporal evolution of the weekly-average number of SWH measurements corresponding to altimeter track crossover positions (typically estimated over several months).
SWH-M-NC-MEAN-GLB	SWH signal monitoring	Significant Wave Height	None	Global map of the averaged along-track SWH (L3) over a month (2x2° grid, for each cell).
SWH-M-NC-STD-GLB				Global map of the standard deviation of along-track SWH (L3) over a month (2x2° grid)
SWH-M-NC-VALID-GLB				Global map of number of along-track SWH valid samples (L3) over a month (2x2° grid)
SWH-M-NC-REJ-GLB				Global map of number of along-track SWH rejected samples (L3) over a month (2x2° grid)

Table 10: List of the metrics used for WAVE-TAC products' operational validation.

IV VALIDATION RESULTS

Validation metrics are used operationally to monitor the quality of the produced significant wave height and wind speed. These metrics are listed in Table 10 and described in detail in the CMEMS-QP-WAVE-ScVP document. In Section IV.1, examples of their application over different time periods are presented.

A filtering process was introduced for the L3 wave products v3.0, section IV.2 presents the improvement with respect to the L2P products.

Assessment of the uncertainties affecting WAVE-TAC products are also completed by specific studies carried out at different steps of the processing, presented in Section IV.3.

Note that the validation for SWOT Nadir is incomplete as at time of writing it has not yet entered into service. This will be addressed when sufficient data is available.

IV.1 Validation and monitoring of significant wave height

IV.1.1 Data availability and spatio-temporal coverage

Figure 7 presents an application of the data availability diagnosis over the period October 15th to 25th, 2018. The upper plot represents the available Level-2P data over the whole period whereas the lower plot represents the missing data. The last day of the period is highlighted in green (absent from the plot on the bottom as it doesn't include this pass). Such a diagnosis on the last day is of great interest in the offline validation process that runs every day.

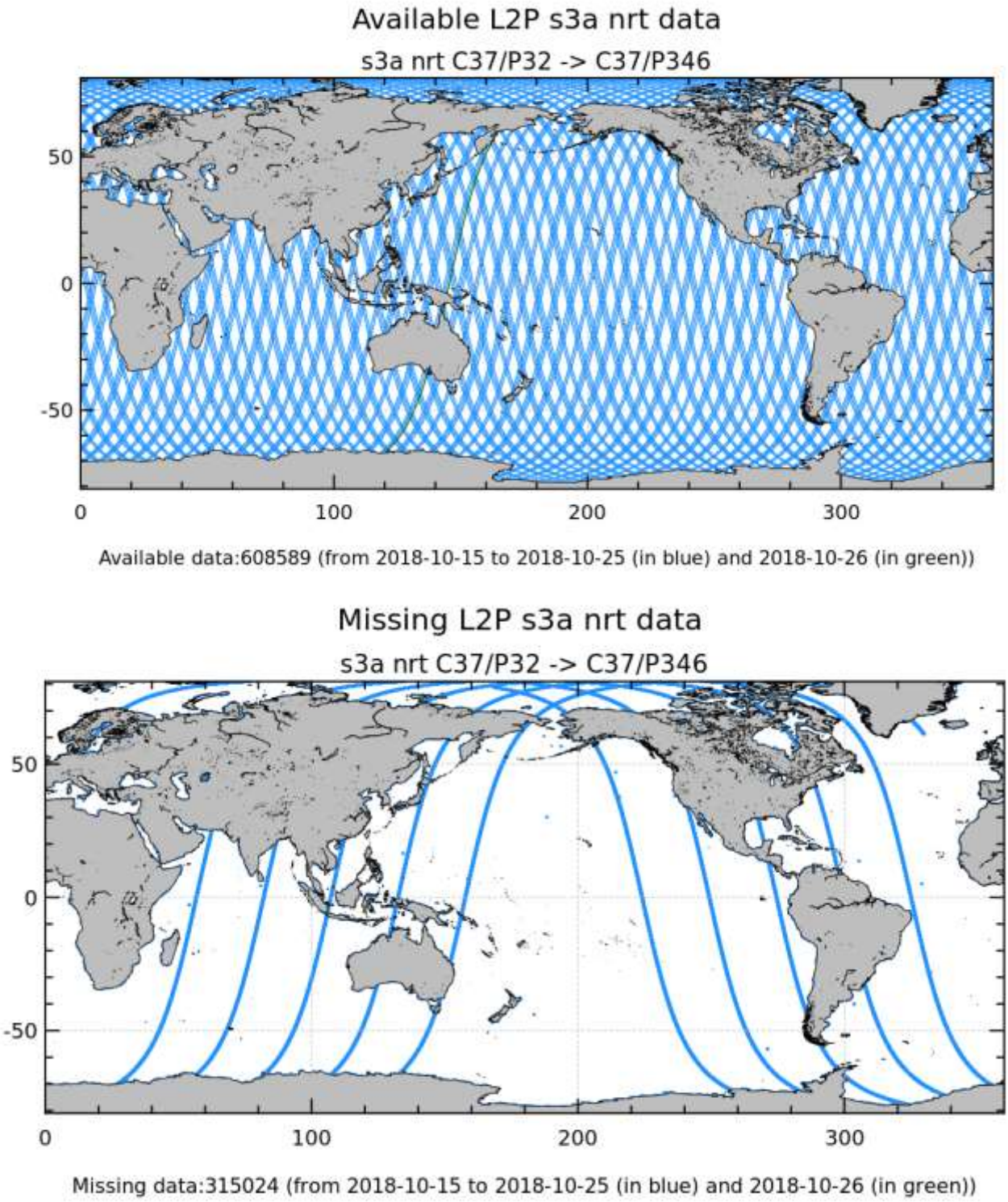

Figure 7: L2 data availability for Jason-3 over the calibration period. Upper: available data. Lower: missing data. Blue = whole period, Green = last day.

IV.1.2 Multi-mission cross-calibration and filtering monitoring

A qualification test of Sentinel-3A's consistency with Jason-3 was performed in order to assess the quality of the calibration over a different period from the one used to establish the cross-calibration. It consists in computing, for each day, the previous 7-day averaged differences between the Sentinel-3A and Jason-3 L3 SWHs at crossover for collocation time interval of 3 hours. As presented in Figure 8, the differences at crossover after calibration (L2P products, red curve) and after calibration and filtering (L3 products with EMD filtering, green curve, or Lanczos filtering, in blue) are centred around zero with daily variations of the order of a few centimetres. This diagnosis allows checking for the consistency between the different missions. The two discontinuities at the beginning of March and in mid-April are explained by a small number of crossover points due to missing Jason-3 data at those dates.

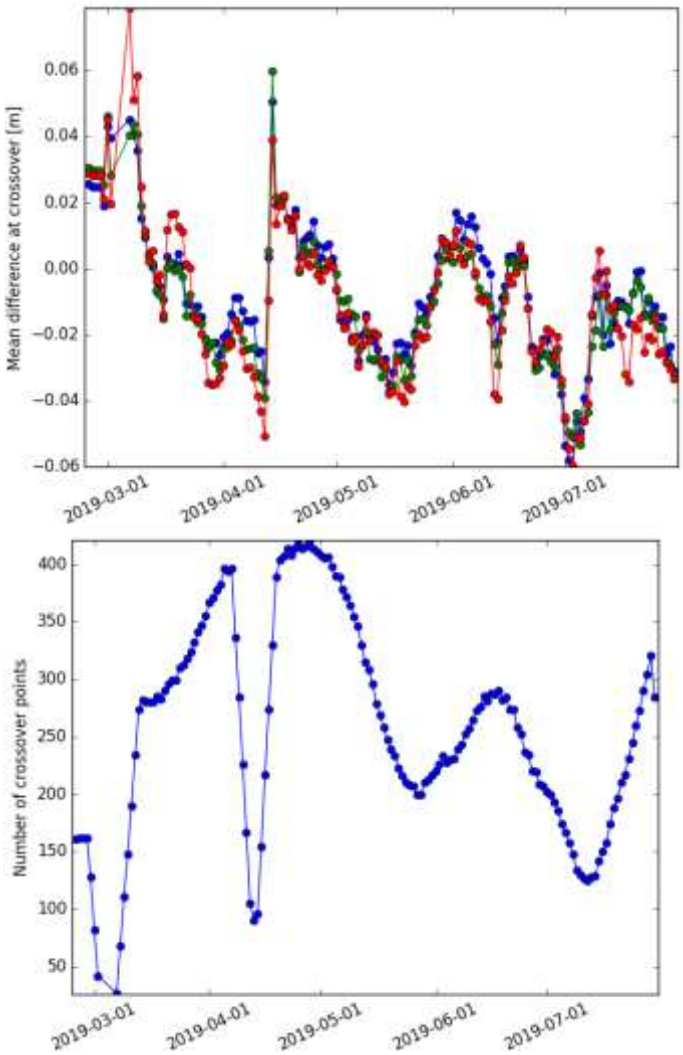

Figure 8: Top: Mean difference at crossover for a 3-hour time constraint. The red curve represents the difference before filtering (i.e. the L2P products). The green and blue curves represent the difference after application of the EMD and Lanczos filters, respectively (corresponding to the v4.0 and v3.0 versions of the L3 products). Bottom: number of 3-hour crossover points.

IV.2 Product quality improvement with along-track filtering

Significant wave height values at crossover between the different missions are used evaluate the noise reduction after filtering.

Figure 9 highlights the performance of the denoising method to reduce the noise for scales < 100 km. Also, it shows that the performance between Sentinel-6A (S6A) and Jason 3 (J3) is very similar, with S6A exhibiting slightly smaller noise plateau both for filtered and unfiltered SWH.

See Section V for a history of all version and calibration changes.

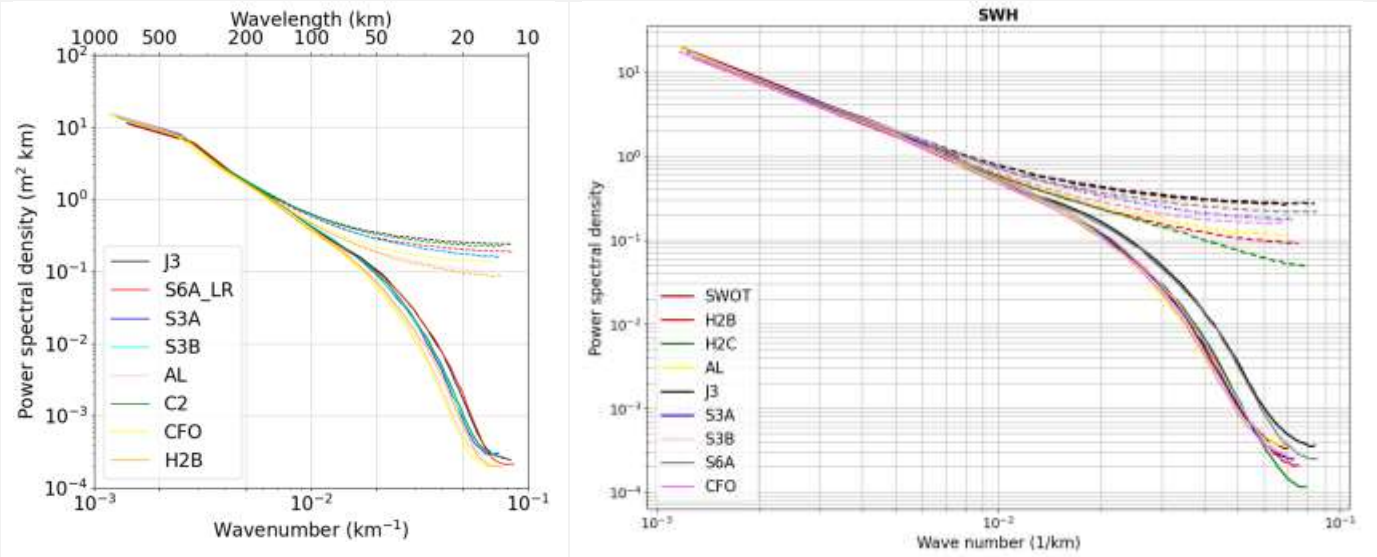

Figure 9: (Left) Power spectra of the SWH measurements for altimeters Jason-3, Sentinel-6A, Sentinel-3A, Sentinel-3B, SARAL/AltiKa, CryoSat-2, CFOSAT and HaiYang-2B over the 83-day period from 25/11/2021 to 16/02/2022. Dashed lines represent the power spectra of the unfiltered SWH data. Solid lines represent the power spectra of the filtered SWH with the EMD method. (Right) Power spectra of the SWH measurements for all altimeters for the validation period of SWOT nadir (from 01-08-2023 to 12-9-2023).

IV.2.1 Distribution of the SWH difference at 3-h crossovers

Time series of the significant wave height differences at crossovers between different missions were computed. A 3-hour time constraint was imposed to ensure that both instruments observed the same sea state. The daily average as well as daily standard deviation were computed (Figure 10 and Figure 11). The filtering does not significantly improve the inter-mission mean bias at crossover (as presented in Table 3 too) but does reduce the standard deviation of the differences at crossovers (Figure 11). This metric reveals how the filters improve the inter-mission consistency of the L3 products, but as this diagnosis mainly probes large scales it does not allow for an accurate comparison of the filtering processes themselves (Lanczos in L3 v3.0 products and EMD in L3 v4.0 products). In section VI more precise diagnoses showing the advantages of the EMD filtering over Lanczos are presented.

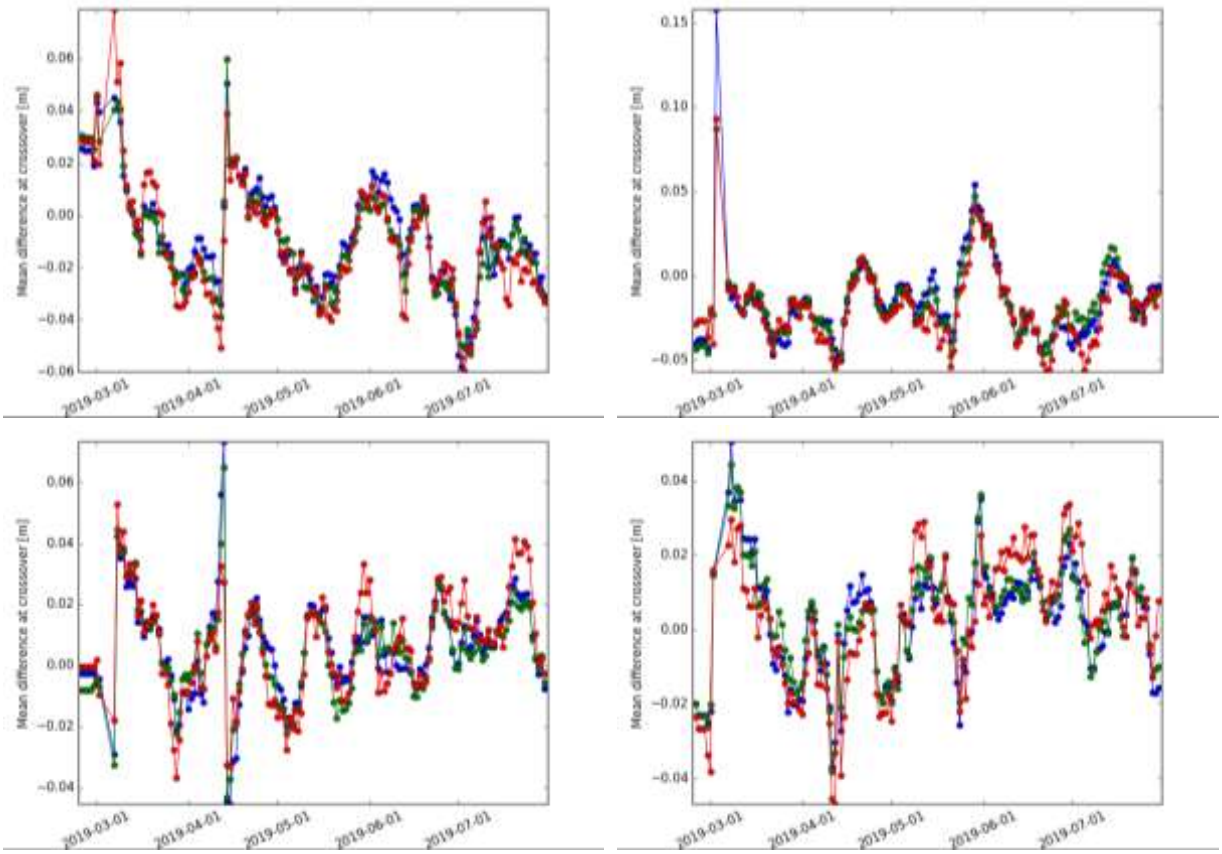

Figure 10: Daily average of SWH difference at crossovers over 7 consecutive days (3-hour constraint). Top left: J3/S3A, Top right: J3/S3B. Bottom left: J3/AL. Bottom right: J3/C2. Red curves: input L2P wave products. Blue curves: L3 wave products with Lanczos filtering. Green curves: new L3 wave products with EMD filtering.

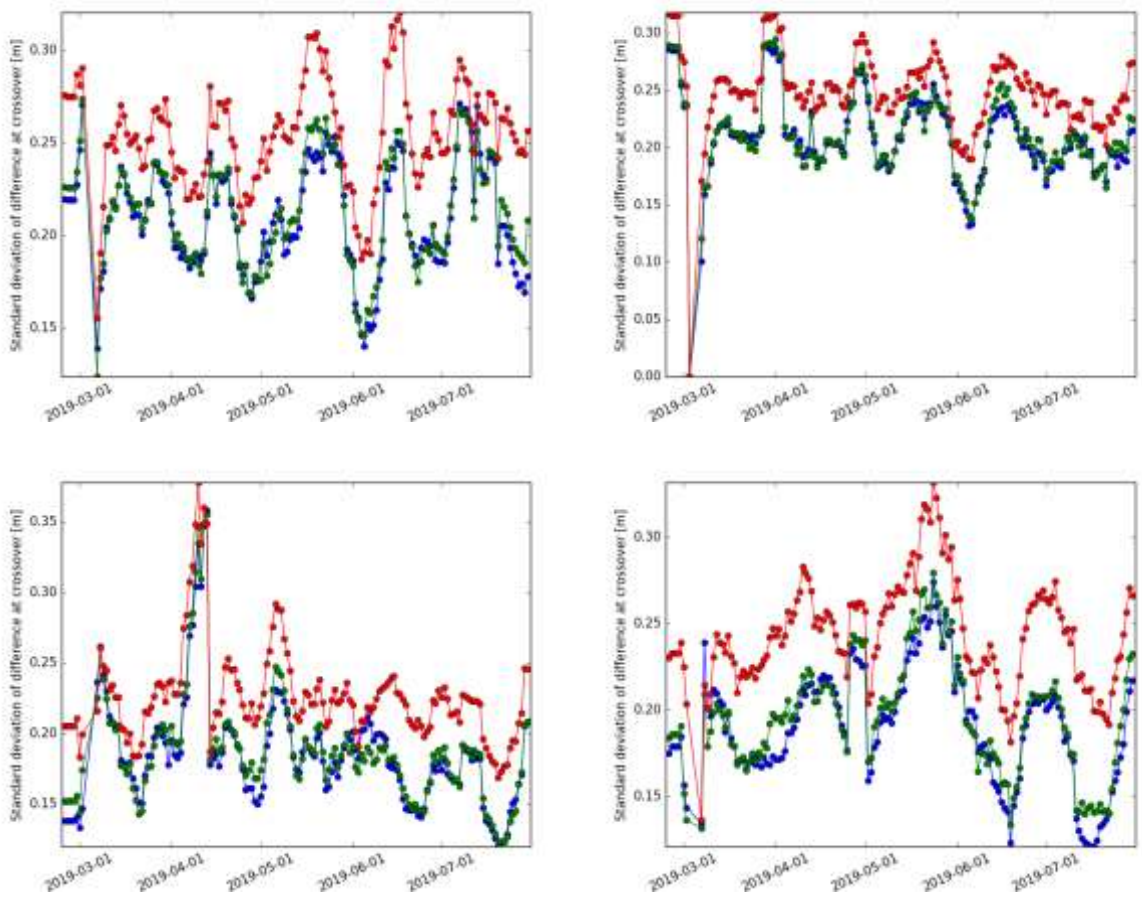

Figure 11: Daily standard deviation of SWH difference at crossovers over 7 consecutive days (3-hour constraint). Top left: J3/ S3A, Top right: J3/S3B. Bottom left: J3/AL. Bottom right: J3/C2. Red curves: input L2P wave products. Blue curves: L3 with Lanczos filtering. Green curves: L3 with EMD filtering.

IV.2.2 Gridded Statistics of the SWH difference at 3-h crossovers

Statistics on the difference between SWH estimates at crossovers are computed within 10°x10° grid cells. The average and standard deviation of these differences are presented in Figure 12 for both L2P and L3 products. The two metrics considered here (mean and standard deviation) show that the agreement at crossovers between the missions is better for the L3 data than for the L2P data.

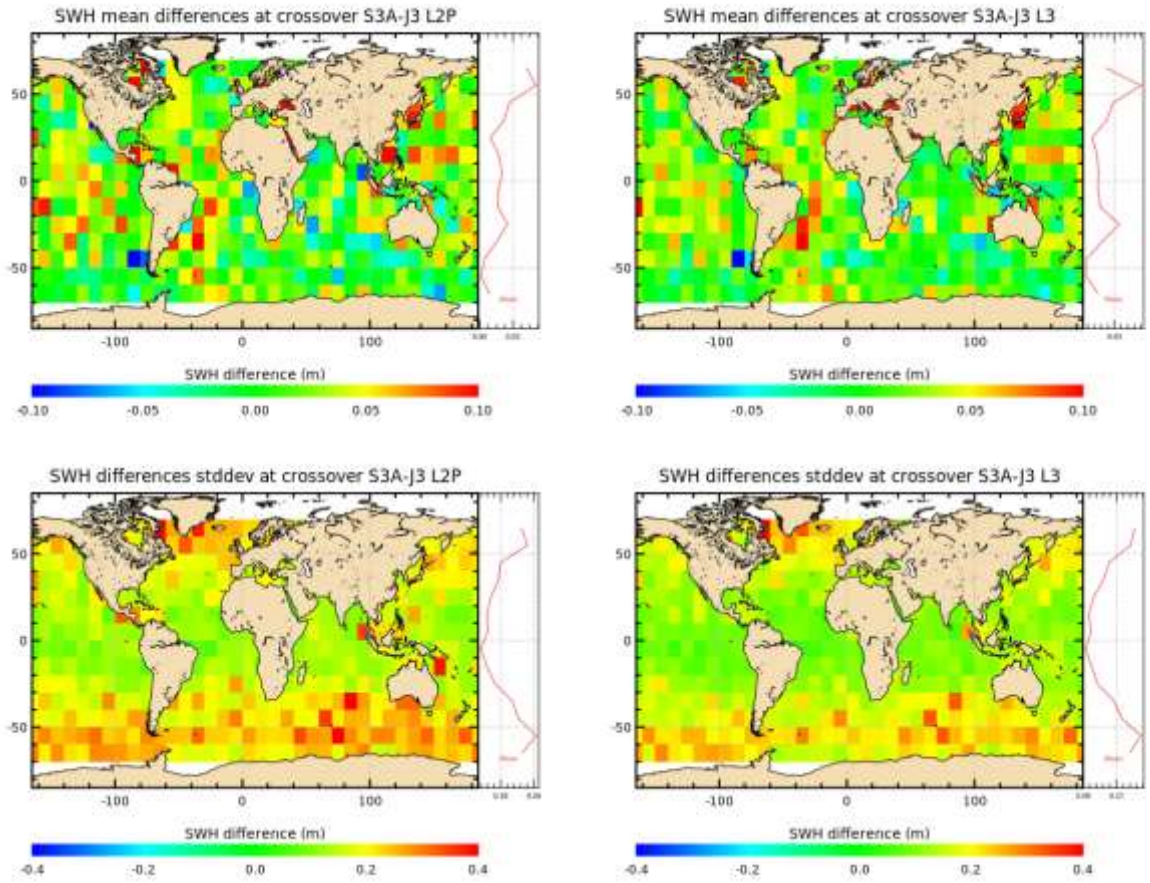

Figure 12: Statistics of SWH differences at 3-h crossover (Sentinel-3A/Jason-3) covering the period from 11th July 2017 to 28th August 2018.

The metrics introduced in sections IV.1 and IV.2 how that the different missions' significant wave height values are in better agreement after application of the filtering algorithm. This indicates that noise on significant wave height measurement is lowered in the L3 products.

IV.3 Additional validation studies to assess processing uncertainties

IV.3.1 Assessment of cross-calibration uncertainties

Calibration of the different missions' significant wave height is done when generating the L2P wave products. As a result, it impacts the L3 wave products. This section provides an estimate of the uncertainties associated with the calibration phase.

IV.3.1.1 Uncertainty associated with the calibration period length

The same AL/J3 cross-calibration process as in Section VII.1.2.1 was performed over a 138-day time period (November 23rd 2016 to April 9th 2017) to obtain an estimate of the uncertainty on the calibration associated with the time period selection (Figure 14). The residual dispersion when considering the fit over the [0-6 m] range increases from 4.1 to 5.5 cm. When comparing both [0-6 m] fits over the two periods, the difference ranges from 0.6 cm for SWH=0 m to 3.2 cm for SWH=12 m, providing an estimate of the uncertainty associated with the calibration period length of the order of a few centimetres for the greatest significant wave heights.

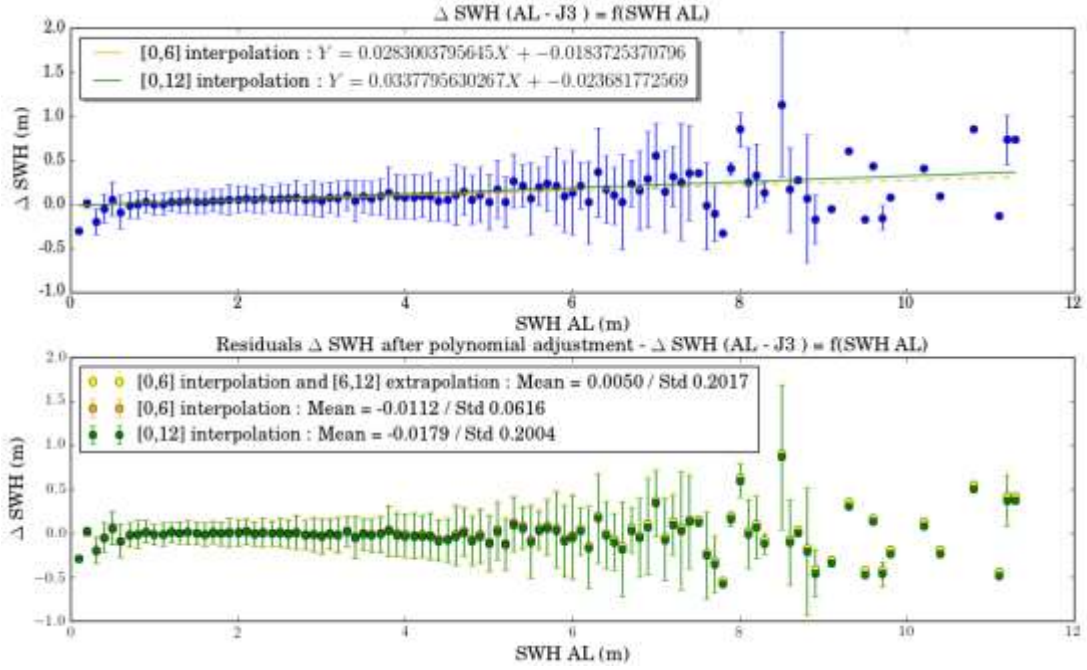

Figure 13: Top: Median of the difference between AltiKa and J3 SWH values at crossover points per 10-cm bin over the period February 17th 2016 - September 14th 2017. Error bars represent the standard deviation of the difference inside each bin. The orange and green curves represent linear fits over different SWH ranges. Bottom: Residuals between the median and the fits.

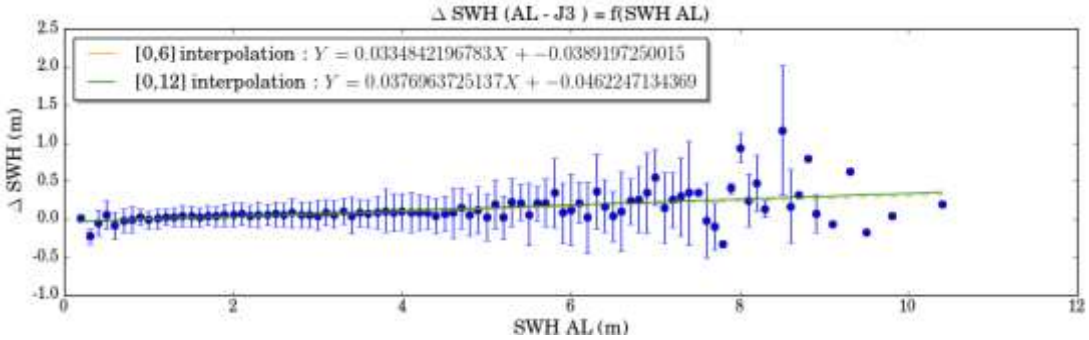

Figure 14: Same as Figure 13 but with a shorter time period: November 23rd 2016 to April 9th 2017.

IV.3.1.2 Uncertainty associated with the crossover time constraint

In Section VII.1.2.2, the crossover calibration between AltiKa and Jason-3 was computed over crossover points collocated with a time constraint of 3 hours. The dependency on the crossover time constraint was assessed by imposing a maximum time difference of 1 hour at crossover. As presented in Figure 15 and Figure 16, this decreases the number of crossover points by a factor of about 3 with respect to a 3-hour time constraint. When comparing the [0-6 m] linear fits using the one- (Figure 17) and 3-hour (Figure 13) time constraints, the difference ranges from 0.4 cm for SWH=0 m to 6 cm for SWH=12 m, providing an estimate of the uncertainty associated with the crossover time constraint of the order of centimetres for the greatest significant wave heights.

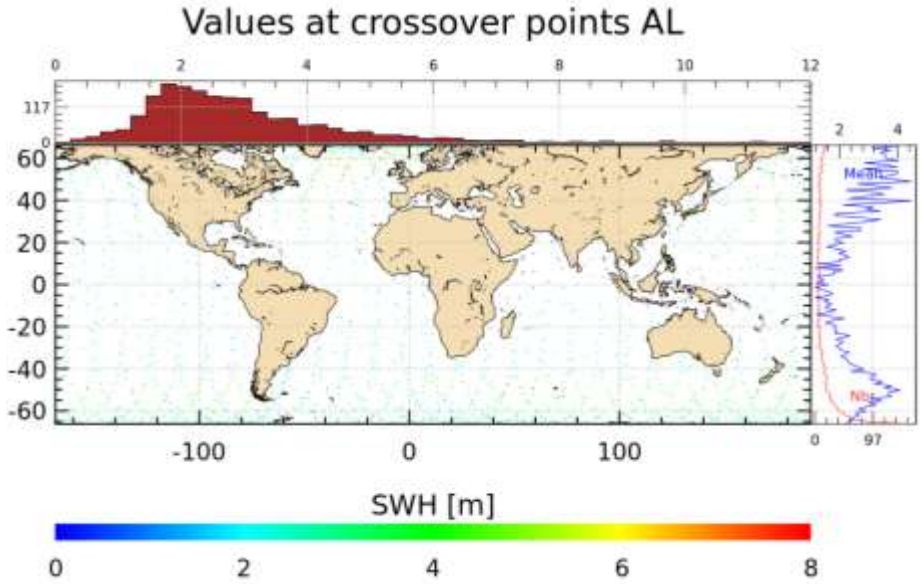

Figure 15: Spatial distribution of AltiKa and Jason-3 crossover points. Only valid points after editing are displayed. Top: histogram of the Altika SWH values of the selected points. Right: Number of points and mean SWH valid values as a function of latitude. February 17th 2016 to September 14th 2017, 1-hour crossover constraint.

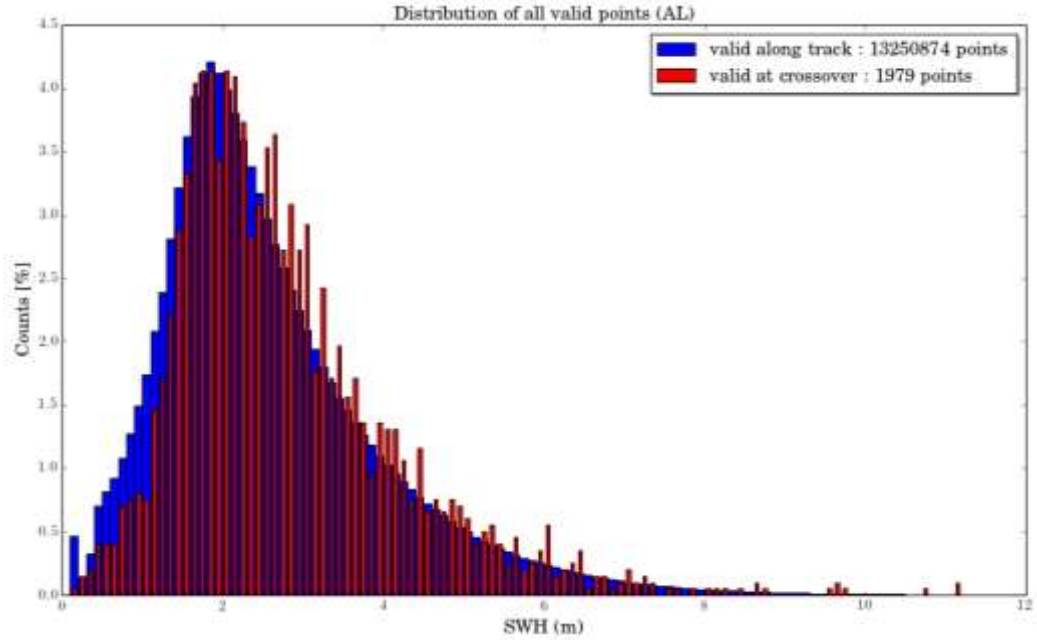

Figure 16: Valid AltiKa SWH distribution over the cross-calibration period (February 17th 2016 to September 14th 2017). 1-hour crossover constraint.

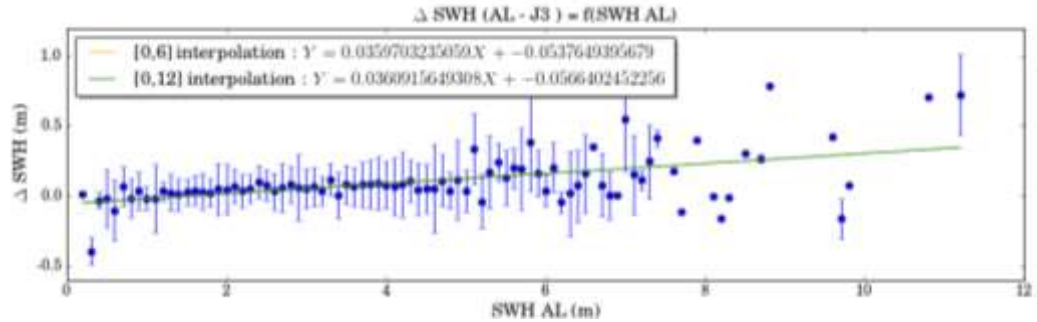

Figure 17: Same as Figure 13 but with a 1-hour crossover time constraint

IV.3.1.3 Uncertainty associated with the cross-calibration method

Other studies carried out a cross-calibration between Jason-3 (J3) and AltiKa (AL). We compare here the results obtained by Queffeulou [2016] with the cross-calibration function used for this study.

Queffeulou [2016] applied some editing criteria based on SWH Root Mean Square (RMS) dispersion and compared AltiKa and Jason-3 significant wave heights over 1-hour collocated cells (Figure 18). Expressing J3 as a function of AL, they obtained the SWH AL calibration correction $H_{corr} = 0.9822\,H - 0.0026$, where H_{corr} and H are the corrected and deduced SWH from AL. The SWH AL calibration correction obtained in the present study with 1-hour crossover points is $H_{corr} = 0.9779\,H - 0.012$ (Figure 19). Their difference spans from 1.5 cm to -3.7 cm over the [0-12 m] range, with 0.6 and -1.1 cm difference at SWHs of, respectively, 2 m and 6 m (0.30% and -0.19% uncertainties). This confirms the excellent agreement between the two studies despite their different periods and point selection criteria.

The bias (defined as the mean of the difference) between the AL and J3 values is 5.4 cm, and the dispersion is 15.6 cm (Figure 19). Queffeulou's results were a J3/AL bias of -5.8 cm and dispersion of 22.7 cm. The biases are in good agreement, though in the present study the dispersion is smaller due to the comparison of the SWHs at crossover while Queffeulou's [2016] values result from collocation within a 1-hour time window, not restricted to the exact crossover position. Adding a 50 km maximum distance criterion, Queffeulou's [2016] mentioned the dispersion reduces to 12-14 cm in agreement with our 15.6 cm dispersion value. Their slightly smaller value may be due to a more restrictive editing that includes stricter criteria on the standard deviation of the high frequency wave height estimates used to compute the 1 Hz significant wave height value.

When using the formula derived from Figure 17 (fit of the difference AL-J3 at 1-hour crossover points), the differences with the Queffeulou [2016] results range from -5.1 cm to -15.8 cm over the [0-12 m] interval, with a 2.1 and -5.1 cm difference at SWHs of 2 and 6 m respectively (1.05% and 0.85% uncertainties). This different fitting method also agrees well with Queffeulou [2016]. This comparison provides us with an estimate of the uncertainty arising from the fitting method (scatter plot VS differences per bin), that is of the order of 5-10 cm. The calibration uncertainty is therefore dominated by the fit method rather than the data selection period length (provided it is long enough) or the temporal constraint (1 or 3 hours) at crossover.

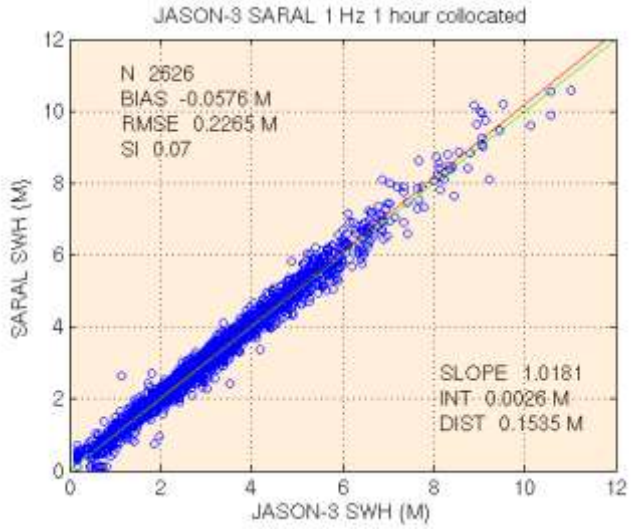

Figure 18: SARAL-AltiKa SWH comparison with Jason-3 for 1 Hz, 1-hour collocated data. From Queffeulou [2016].

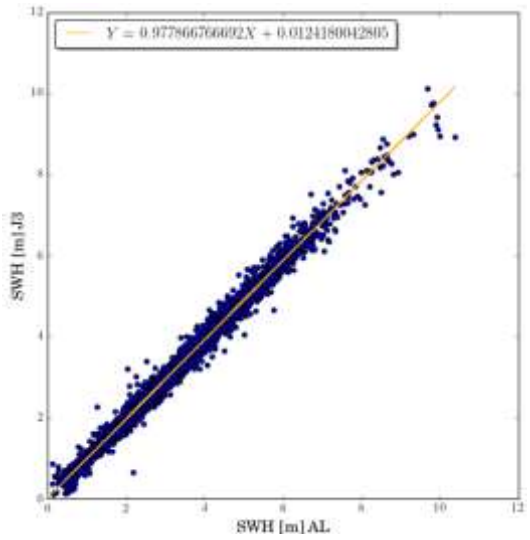

Figure 19: SARAL-AltiKa SWH comparison with valid 1 Hz Jason-3 measurements at crossover points within a 1-hour interval. Mean difference between the AL and J3 values is 5.36 cm with a 15.6 cm dispersion.

V SYSTEM'S NOTICEABLE EVENTS, OUTAGES OR CHANGES

This section is dedicated to track and describe changes that may occur in the current operational system: due to outages, version or upstream data changes (e.g., addition or loss of a satellite). The main changes in the versions of the L3 alti wave operational system are described in table 11.

V.1 System version changes

System version	Date of Entry in Service of the change	Description of the change	Impact on product quality?
V1.0	11/07/2017	Entry into Service of the L3 alti wave chain with Jason-3 and Sentinel-3A missions	Yes
V1.1	02/10/2017	New calibration procedure to account for L2 input data versioning (anticipation of future L2 version changes)	No
V1.2	29/01/2018	Integration of SARAL/AltiKa mission Improvement of S3A / J3 cross-calibration correction	Yes
V2.0	03/07/2018	Integration of Cryosat2 mission Changes in the format (Netcdf4, new attributes, change of SWH fill value)	Yes
V3.0	16/04/2019	Integration of filtering process, Evolution in the file covering period: from 1 pass to 3-hour period, new L2P upstream data with enhanced data editing; Integration of Sentinel-3B mission	Yes
V4.0	03/12/2019	Evolution of the filtering process from Lanczos to EMD based method. Add the unfiltered SWH field in the products. New CFOSAT L3 products	Yes
V5.0	07/07/2020	Integration of HaiYang-2B mission, addition of collocated wind field	Yes
V5.1	08/04/2021	Upgrade of the wind algorithms for Sentinel-3 missions.	Yes
V5.2	05/04/2022	Integration of Sentinel-6A mission. Temporary interruption of Jason-3 dataset while changing orbit (until ~June 2022)	Yes
V6.0	29/11/2022	Recalibration of Jason 3 SWHs against in situ measurements.	Yes
V7.0	29/11/2023	Integration of SWOT nadir mission	Yes

Table 11: L3 alti wave chain version changes.

V.2 Main constellation events impacting data availability and quality

Different events can lead to a change in data availability and quality. Such events are usually:

- A change in the altimeter constellation: the loss or introduction of an altimeter in the constellation directly impacts the number of altimeter measurements available.
- For a specific platform, a reduction in the number of altimeter measurements available as input to the L3 alti wave processing system. This can be linked to an anomaly onboard the platform

or in the ground segment, preventing data reception and impacting the processing steps from L0 to L2P. It can also be caused by abnormal data acquisition in the L3 alti wave system.

- An increase of invalid measurements fed into the L3 alti wave system. This is usually linked to specific platform events (e.g., manoeuvres) but can also be caused by L0-L2P processing anomalies or specificities. In some rare cases, abnormal acquisition by the L3 alti wave system can also lead to abnormal data selection.
- A change in the L0 - L2P processing can lead to changes in the quality of the input measurements to the L3 alti wave system. For example, new versions of L2 upstream products are regularly released, to account for state-of-the-art corrections and developments of this upstream processing.

Currently, ten altimeters constitute the altimeter constellation available in NRT.

- Sentinel-6A (S6A) is the reference mission since April 2022
- Jason-3 (J3) (former reference mission, until April 2022)
- Sentinel-3A (S3A)
- Sentinel-3B (S3B)
- SARAL-DP/AltiKa (AL)
- Cryosat-2 (C2)
- CFOSAT (CFO)
- HaiYang-2B (H2B).
- HeiYang-2C (H2C)
- SWOT nadir (SWOT)

Table 12 summarizes the main events affecting data availability in the NRT product.

Date	Platform	Event
11/07/2017	J3, S3A	Introduction of Jason-3 and Sentinel-3A missions in the L3 wave alti chain
13/12/2017	S3A	New version of the Sentinel-3A L2 production chain (IPF 6.10)
29/01/2018	AL	Introduction of SARAL/AltiKa mission in the L3 wave alti chain
03/07/2018	C2	Introduction of Cryosat2 mission in the L3 wave alti chain
16/04/2019	J3, S3A, S3B, AL, C2	Introduction of Sentinel-3B mission. New L2P upstream data including an enhanced data editing.
03/12/2019	CFOSAT	Introduction of CFOSAT mission in the L3 wave alti chain
07/07/2020	H2B	Introduction of HaiYang-2B mission in the L3 wave alti chain
05/04/2022	S6A, J3	Introduction of Sentinel-6A mission in the L3 wave chain. Interruption of Jason-3 dataset while changing orbit
25/04/2022	J3	Reactivation of Jason-3 mission on an interleaved orbit with S6A
29/11/2022	H2C	Introduction of HaiYang-2C in the L3 wave chain.
29/11/2023	SWOT	Introduction of SWOT nadir in the L3 wave chain

Table 12: Main events affecting the data availability in NRT conditions.

V.3 Historical changes and potential impact for users

V.3.1 October 2017 – System v1.1: new calibration procedure to account for L2 input data versioning

As evolutions can be brought to the upstream L2 production chain, a different cross-calibration correction may be required to ensure consistent performances of L3 products. The computation of this correction requires an early and simultaneous access to the new and previous versions of L2 data in order to determine a new cross-calibration correction between the two L2 versions. This correction is added to the existing correction computed from the cross-calibration with the reference mission. To simplify the change or addition of new calibrations, the L3 alti wave chain was modified to use a lookup table, providing the calibration to be applied as a function of both SWH and L2 file version. The resolution of the lookup table's SWH bins is 5 cm. This version v1.1 of the L3 alti wave chain was implemented in October 2017, in order to anticipate a new version of the Sentinel-3A L2 production chain (detailed in paragraph V.3.2). The implementation of this new version has no impact on the production.

V.3.2 December 2017 – New version of Sentinel-3A L2 production chain (IPF6.10)

A new version of the Sentinel-3A L2 production chain (IPF 6.10) is operated at European Organisation for the Exploitation of Meteorological Satellites (EUMETSAT)since December 13th, 2017 in replacement of the IPF 6.07 version. The 6.10 version presents a modification in the SAMOSA retracking with respect to v6.07, impacting the SAR significant wave height. Consequently, the calibration correction embedded in the L3 alti wave chain was updated to account for this IPF version change.

Valid SWH values from both IPF versions were compared during a 20-day period. As all points from IPF v6.10 and IPF v6.07 are collocated, a 20-day period is long enough to perform the cross-calibration. The significant wave height bias between the two L2 versions is presented on Figure 20. A second-order polynomial function is fitted to this bias and added to the existing Sentinel-3A calibration correction lookup table.

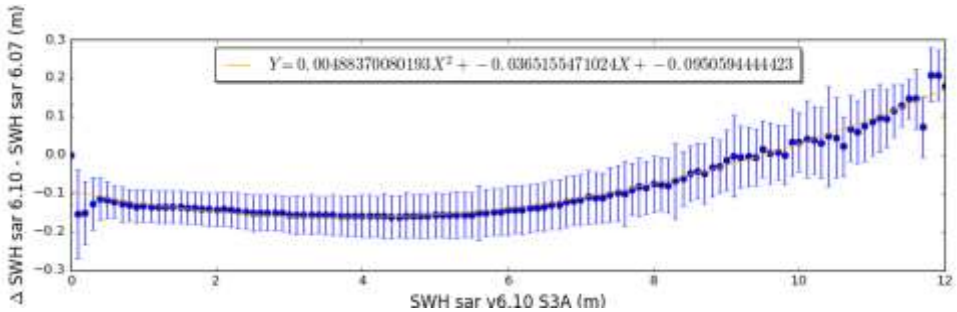

Figure 20: Differences between the IPF versions v6.10 and v6.07 of L2 S3A SAR significant wave height before polynomial adjustment.

This joint upgrade of L2 IPF version and L3 alti wave chain (from v1.0 to v1.1) has little impact on the produced Sentinel-3A L3 data. We plotted the differences between L3 SWH produced with IPF v6.07 L2 and v1.0 L3 chain and L3 produced with IPF v6.10 L2 and v1.1 L3 chain over one day (Figure 21). Observed bias is due to the use of a lookup table in the new v1.1.0, that induces small differences due to the

interpolation in-between the values provided by the lookup table. However, the introduced differences remain smaller than 1 cm.

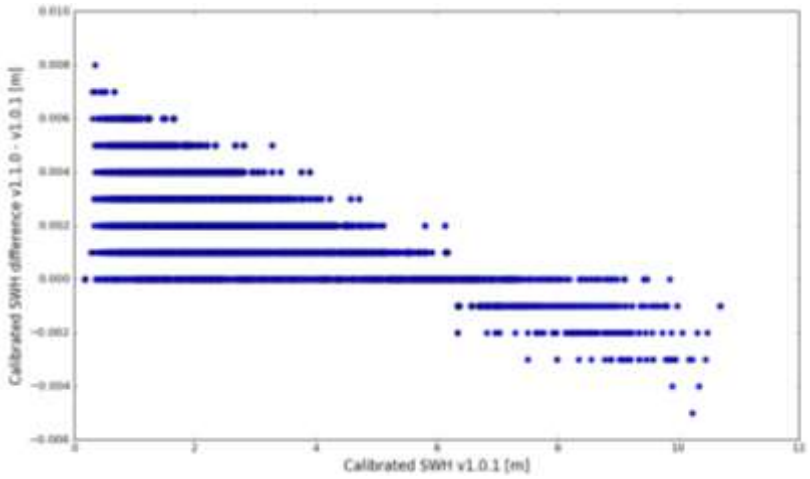

Figure 21: Differences of the S3A intercalibrated SWH in the L3 products with respect to the previous version of the processing chain as a function of the significant wave height.

V.3.3 January 2018 – System v1.2: introduction of AltiKa mission and Improvement of S3A / J3 cross-calibration

Calibration and validation of AltiKa mission is detailed in Section VII.1.2.

Monitoring and quality control of the v1.0 L3 chain production highlighted a small residual bias of the order of 5 cm between Sentinel-3A (IPF v6.07) and Jason-3 as illustrated on Figure 22 (left). Investigation showed that the cross-calibration formula between Sentinel-3A PLRM and Jason-3, determined initially over the [0-12 m] range (see *Figure 22*,green curve), presented a decrease in accuracy over the [0-6 m] range where most of the wave population lies. Therefore, the cross-calibration linear correction between Sentinel-3A PLRM and Jason-3 is now computed over the [0-6 m] range .

The cross-calibration second order polynomial adjustment used to cross-calibrate Sentinel-3A PLRM and SAR (IPF 6.07 version) significant wave heights was also modified to avoid being impacted by the [0-1 m] data, showing large discrepancies compared to the [1-12 m] bias distribution. Initially computed over the [0-12 m] range ($Corr = -0.0108\,H^2 + 0.126\,H - 0.0345$), it is now determined over the [1-12 m] range ($Corr = -0.0105\,H^2 + 0.122\,H - 0.0225$).

After applying the new calibration, the mean difference at crossover between S3A and J3 L3 significant wave heights is very close to zero (Figure 22, right).

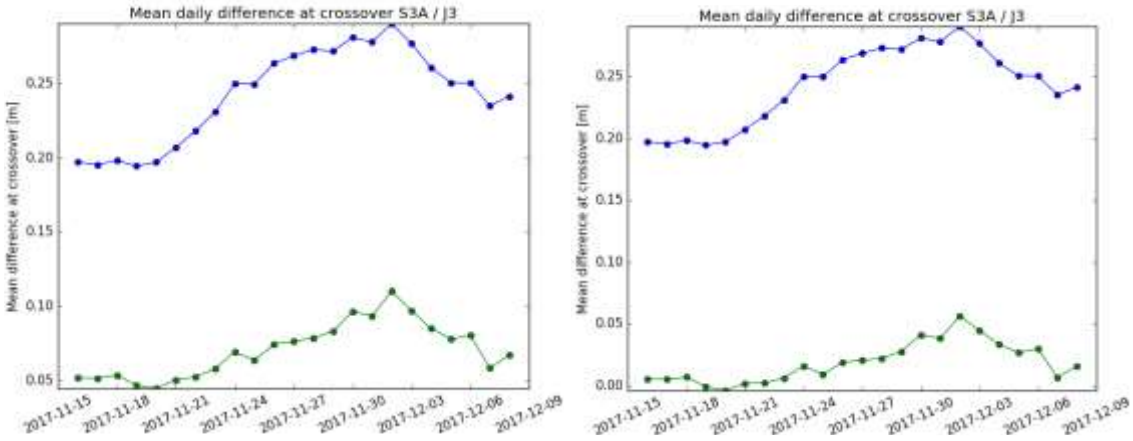

Figure 22: Mean difference at crossover for a 3-hour time constraint (left) before improving S3A / J3 cross-calibration (system v1.1) and (right) after (system v1.2). Blue curve represents the difference before calibration (as in the L2 products). The green curve represents the difference after calibration (as in the L3 products).

V.3.4 July 2018 – System v2.0: introduction of Cryosat2 mission

Calibration and validation of Cryosat mission is detailed in Section VII.1.2.

No calibration changes were implemented regarding the other missions.

V.3.5 April 2019 – System v3.0: Quality and format evolutions of L3 products, new input, introduction of Sentinel-3B mission

The L3 alti wave chain was updated with:

- a new along-track filtering algorithm (described in sections II.4.2), improving significantly the mean and standard deviation of the SWH differences at cross-overs (see section IV.2).
- a new temporal sampling: a file now covers 3 hours of measurements
- new upstream data: L3 data are now processed using the internally processed L2P data. Those L2P are described in section VII. The main change from previous versions is an enhanced data editing of invalid points
- a new mission: Sentinel-3B L3 products are now available (cross-calibration is presented in section VII.1.2.2).

V.3.6 December 2019 – System v4.0: Evolution of the filtering method, introduction of CFOSAT mission

The L3 alti wave chain was updated with:

- a new along-track filtering algorithm (described in sections II.4.2), based on the EMD technique
- a new mission: CFOSAT L3 products are now available
- addition of the VAVH_UNFILTERED field in the NetCDF products

V.3.7 July 2020 – System v5.0: Addition of collocated altimetry wind field, introduction of HaiYang-2B mission

The L3 alti wave chain was updated with:

- a new wind field derived from altimeter measurements and intercalibrated on Jason-3 reference mission
- a new mission: HaiYang-2B L3 products are now available

V.3.8 April 2021 – System v5.1: Update to Jason-3 GDR-F standard and update of wind speed algorithm for Sentinel-3 missions

This update only impacts the collocated wind speed and not the significant wave height. All missions are impacted. The two upgrades of upstream data are described hereafter:

- Update to Jason-3 GDR-F standard

The wind speed is calculated through a mathematical relationship with the Ku-band backscatter coefficient and the significant wave height using the Gourrion approach [Gourrion et al, 2002] and Collard's model computed from Jason-1 data [Collard, 2005]. The standard of Jason-3 Level-2 data has been upgraded from GDR-D to GDR-F, with noticeable changes in the backscatter coefficient. This upgrade results in a bias between GDR-F and GDR-D wind speed values.

As Jason-3 is the reference mission, all missions are now cross-calibrated onto the new GDR-F standard of Jason-3. Collocated wind speed values are therefore expected to increase by up to 0.5 m/s for values of wind speed larger than 5 m/s.

- Update of wind speed algorithm for Sentinel-3 missions

The wind speed of Sentinel-3 missions was previously calculated through a one-dimensional wind speed model, as a function of backscatter only, using Abdalla's approach [Abdalla 2007]. A two-dimensional model, as a function of backscatter and significant wave height, is now used to compute the wind speed. As for Jason-3, it is based on Gourrion approach [Gourrion et al, 2002] and Collard's table [Collard, 2005] with pseudo-Low-Resolution Mode (PLRM) backscatter and significant wave height.

V.3.9 April 2022 – System v5.2: Integration of Sentinel-6A as the new reference mission, change of orbit of Jason-3

The Copernicus mission Sentinel-6A is integrated in the L3 alti wave chain. Sentinel-6A replaces Jason-3 as the reference mission. The Jason-3 and Sentinel-6A missions were on a tandem orbit until April 2022. Jason-3 orbit change manoeuvres were carried out in April 2022 and during this period, the dataset was temporarily unavailable. Jason-3 has been available again since reaching its new orbit.

Sentinel-6A being the new reference mission means that it is now the reference for the monitoring of biases at crossovers with other missions.

In the future, when a new mission is integrated (as is the case with HaiYang-2C), Sentinel-6A will be the reference for the calculation of the cross-calibration of SWH and wind speed.

V.3.10 November 2022 – System v5.3: New calibration of Jason-3 against in situ data

Jason-3 was recalibrated against in situ data, and a new lookup table produced by Dodet and Piollé (2021). This new absolute calibration replaces the old linear fit determined by Queffeulou and Croizé-Fillon (2017). There are two advantages to this new calibration: the first is that the previous one was calculated for Jason-2, for at the time the record for Jason-3 was not long enough to permit an independent calibration; now Jason-3's record is sufficiently long to produce its own, independent calibration. The second is that a lookup table is sensitive to non-linearities in the correspondence between the in situ and altimetric measurements, whereas the linear function, by definition, was not.

Although Sentinel-6a is the new reference mission, until such a time as a sufficiently long record exists to permit a new calibration, it will be cross-calibrated with Jason 3 the same as any other secondary mission. However future missions that cannot be cross-calibrated with Jason-3 will be cross-calibrated with Sentinel-6 (which is itself cross-calibrated with Jason-3, which in turn has been calibrated against in situ data).

The new absolute calibration leads to differences from the preceding one which depends on the mission. For example, Figure 23 shows the regional differences for Sentinel-3A. We can see an impact for low and high waves. A more exhaustive validation is done in section VI to present and assess the quality of the new calibration.

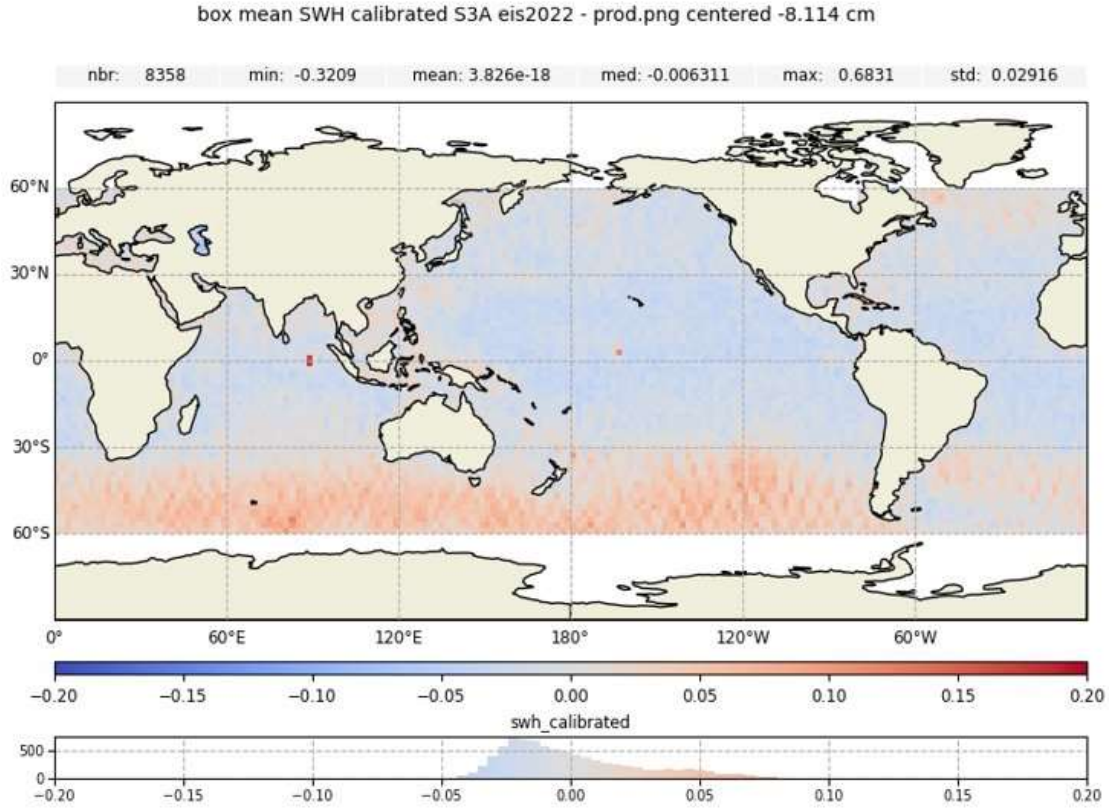

Figure 23: Differences of L2P SWH calibrated for Sentinel-3A between the two calibration versions (reference mission with linear fit vs look up table against in situ measurements).

VI QUALITY CHANGES SINCE PREVIOUS VERSION

The Copernicus mission Sentinel-6A is integrated in the L3 alti wave chain. Sentinel-6A replaces Jason-3 as the reference mission. Jason-3 and Sentinel-6A missions were flying on the same orbit until April 2022. Jason-3 was manoeuvred into a new orbit in April 2022 and during this period the data record is empty. The record resumed after reaching its new orbit.

Sentinel-6A being the new reference mission means that it is now the reference for the monitoring of biases at crossovers with other missions.

In the future, when a new mission will be integrated (such as HaiYang-2C), Sentinel-6A will be the reference for the calculation of the cross-calibration of SWH and wind speed.

Figure 24 shows the power spectra of SWH for the different altimeter missions over a common period. It highlights that Sentinel-6A LR filtered wave measurements show a performance similar to existing missions.

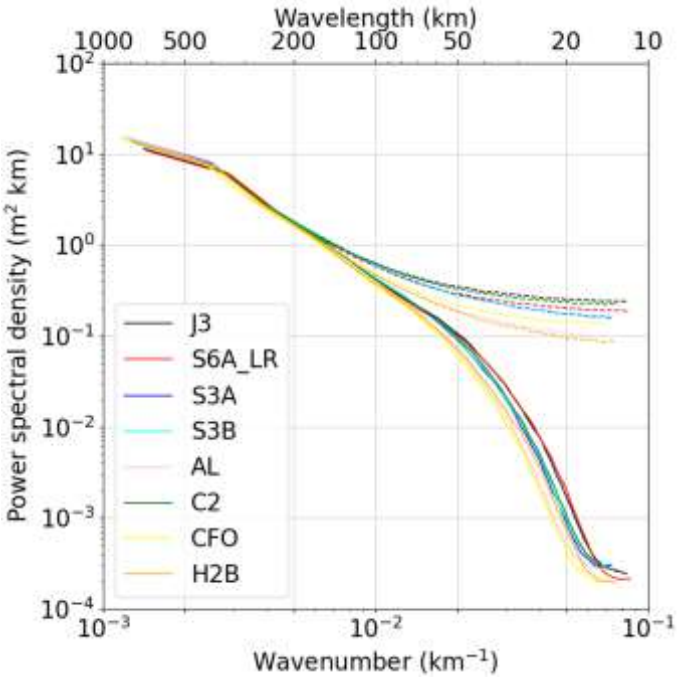

Figure 24: Power spectra of altimeter SWH measurements over the period 25th November 2021 to 16th February 2022. Dashed lines represent the power spectra of the L2P 1 Hz calibrated SWH data. The solid lines represent the power spectra of the L3 1 Hz data filtered with the EMD method.

VII APPENDIX INPUT L2P PRODUCT SPECIFICITIES

This section describes the upstream L2P products used to generate the L3 products distributed in CMEMS catalogue. Upstream L2P products are generated in an independent wave chain. The main steps are the editing of L2 data, the cross-calibration and the absolute calibration with respect to buoys. This section details those main processing steps as they are important to better assess the quality of the final L3 products.

VII.1.1 Data editing

VII.1.1.1 Editing criteria

Quality Control on the input L2 data is a critical process applied to guarantee that the system uses only the most reliable altimeter data. The L2P system is supplied with L2 products that contain data directly derived from altimeter measurements (e.g., range, sigma0, etc.) as well as geophysical data (e.g., dry tropospheric correction, significant wave height, etc) and flags (e.g., surface type, ice presence, etc.). These values are provided at high (20 Hz for Jason-3) and low (1 Hz) frequency. Only the 1 Hz data are used in the L3 alti wave system.

Data are selected as valid or invalid using a combination of various criteria such as quality flags and parameter thresholds (see Table 13 for details). These criteria are adapted from the ones used for the Sea Level Anomaly (e.g., Aviso/SALP 2016), except for CFOSAT that has a specific editing. Only criteria related to retracking derived values were selected. Geophysical parameters (e.g., tropospheric corrections) do not intervene in the SWH estimation. For Sentinel-3A, Sentinel-3B and Cryosat2, the criteria on the off-nadir angle are not activated since this value is not derived from the retracking in SAR mode and therefore its value does not provide information about data quality.

Parameter	Method	Sentinel-6A LR	Jason-3	Sentinel-3A Sentinel-3B SAR	AltiKa	Cryosat2	CFOSAT	HaiYang-2B	HaiYang-2C	SWOT nadir
Ice Flag	Flag	Ice flag =0, based on OSI SAF	Valid value: 0	Valid value: 0 or 5	Valid value: 0	Ice flag =0, based on OSI SAF	Ice flag=0, based on ECMWF	Valid value: 0 or 5	Valid value: 0 or 5	Valid value: 0
Surface type Flag	Flag	Valid value: 0 or Caspian Sea (2 & basin=22)	Valid value: 0 or Caspian Sea (2 & basin=22)	Valid value: 0 or Caspian Sea (1 & basin=22)	Valid value: 0 or Caspian Sea (1 & basin=22)	Valid value: 0 or Caspian Sea (1 & basin=22)	Valid : 0	Valid value: 0 or 1	Valid value: 0 or 1	Valid value: 0 or Caspian Sea (2 & basin=22)
Swh [m]	Threshold	Min: 0 max: 30	Min: 0 max: 30	Min: 0 Max: 30	Min: 0 Max: 30	Min: 0 Max: 30	Min: 0 Max: 30	Min: 0 Max: 30	Min: 0 Max: 30	Min: 0 max: 30
Sigma0 [dB]	Threshold	Min: 5 Max: 28	Min: 9.38 max: 32.38	Min: 5 Max: 28	Min: 3 Max: 30	Min: 2.8 Max: 30	Min: 5 Max: 25	Min: 5 Max: 28	Min: 5 Max: 28	Min: 9.38 max: 32.38
Square off-nadir angle	Threshold	N/A	Min: -0.2 max: 0.64	N/A	Min: -0.2 Max: 0.0625	N/A	N/A	N/A	N/A	Min: -0.2 max: 0.64
Wind speed [m/s]	Threshold	Min: 0 Max: 30	Min: 0 Max: 30	Min: 0 Max: 30	Min: 0 Max: 30	Min: 0 Max: 30	Min: 0 Max: 30	Min: 0 Max: 30	Min: 0 Max: 30	Min: 0 Max: 30
Orbit - range [m]	Threshold	Min: -130 Max: 100	Min: -130 Max: 100	Min: -130 Max: 100	Min: -130 Max: 100	Min: -130 Max: 100	N/A	Min: -130 Max: 100	Min: -130 Max: 100	Min: -130 Max: 100
Sigma0 standard deviation [dB]	Threshold	Min: 0 Max: 0.7	Min: 0 Max: if distance to shoreline <50 km: 2.5 else:1	Min: 0 Max: 0.7	Min: 0 Max: 1	Min: 0 Max: 1	Min: 0 Max: 2	Min: 0 Max: 0.7	Min: 0 Max: 0.7	Min: 0 Max: if distance to shoreline <50 km: 2.5 else:1
Range standard deviation [m]	Threshold	Min: 0 Max: if SWH<2: 0.192 else: 0.018*SWH +0.156	Min: 0 Max: 0.0115*SWH+ 0.2	Min: 0 Max: 0.02*SWH +0.12	Min: 0 Max: 0.2	Min: 0 Max: 0.013*SWH+0. 2 (LRM) / 0.014*SWH+0. 25 (SARM)	N/A	N/A	N/A	Min: 0 Max: 0.0115*SWH+ 0.2
swh_numval	Threshold	Min: 18	Min: 10	Min: 18	Min: 20	Min: 10	N/A	Min: 18	Min: 18	Min: 10
swh_RMS	Threshold	Min: 0 Max: f(swh)	Min: 0 Max: f(swh)	Min: 0 Max: f(swh)	Min: 0 Max: f(swh)	Min: 0 Max: f(swh)	Min: 0 Max: f(swh)	Min: 0 Max: f(swh)	Min: 0 Max: f(swh)	Min: 0 Max: f(swh)

Table 13: Flag and threshold editing criteria for the different missions.

These editing criteria were applied to data covering a 25-day period between 2018 October 4th and 2018 October 26th.

The resulting percentages of rejected measurements are provided in Table 14. The very low rejection level due to the surface type flag on S3-A and S3-B SAR data is because the ocean-only Sentinel-3A&B products are used. S3 land and ocean products overlap only slightly, of the order of 300 km, explaining the low 2% rejection level due to the surface type. Edited measurement percentage is higher for AltiKa and Cryosat2, which is a result of their coverage at higher latitudes (respectively 81.5° and 88° N/S compared to 66°N/S for Jason-3), inducing a higher percentage of ice and surface type flags. Statistics provided for Cryosat2 contain both SAR and LRM data. Due to its specific editing, the percentages of the edited values for each criterion are consequently very different from those of the other missions. The total percentage of edited measurements over oceans (19.40%) is of the same order of magnitude as for Sentinel-3A and 3B.

Thanks to the high quality of current missions, the threshold criteria reject a small percentage (about 4 to 7%) of altimeter measurements for all missions. The percentage of threshold edited measurements is expected to present an intra-annual variability of a few tenths of a percent, as seen in CalVal studies.

Parameters	Jason-3	Sentinel-3A SAR	Sentinel-3B SAR	AltiKa	Cryosat2	CFOSAT
Ice Flag	21.88	13.95	13.93	27.15	9.63	17.21
Surface type Flag	29.48	2.37	2.39	32.47	28.16	12.14
Combined Flags	**38.32**	**16.31**	**16.31**	**42.59**	**37.33**	**N /A**
Swh	0.55	0.04	0.05	0.28	0.54	12.14
Sigma0	0.58	0.13	0.18	0.32	0.6	16.31
Square off-nadir angle	0.63	N/A	N/A	0.29	N/A	N/A
Wind speed	1.22	0.04	0.05	0.28	1.49	16.37
Orbit - range	0.83	0.06	0.12	0.45	1.0	N/A
Sigma0 standard deviation	1.95	2.87	2.99	0.96	1.21	14.74
Range standard deviation	0.73	1.33	1.40	1.42	1.05	N/A
Minimum number of high frequency values	1.14	0.37	0.44	1.08	5.49	N/A
Threshold on swh_RMS	1.73	3.12	3.18	3.76	1.38	13.94
Combined thresholds	**3.82**	**4.57**	**4.74**	**4.69**	**7.30**	**N/A**
All criteria	**40.68**	**20.14**	**20.28**	**45.28**	**41.92**	**19.40**

Table 14: Percentage of rejected measurements estimated for Jason-3, Sentinel3-A, Sentinel-3B, AltiKa and Cryosat2 over 25 days between 2018 October 4th and 2018 October 26th. For CFOSAT statistics were obtained on 13 days over cycle 21.

The following figures give an example of the editing spatial distribution for one day. Figure 25 shows the input L2 SWH values (top) and the output L3 SWH values (bottom) for Jason-3. As visible in Figure 26, most of the edited SWH values are located on land or ice (in yellow) and only few values are edited with the threshold criteria (in red). Finally, Figure 27 shows the SWH timeseries for one day, before and after editing. The edited blue curve is exempt from outliers and unphysical values.

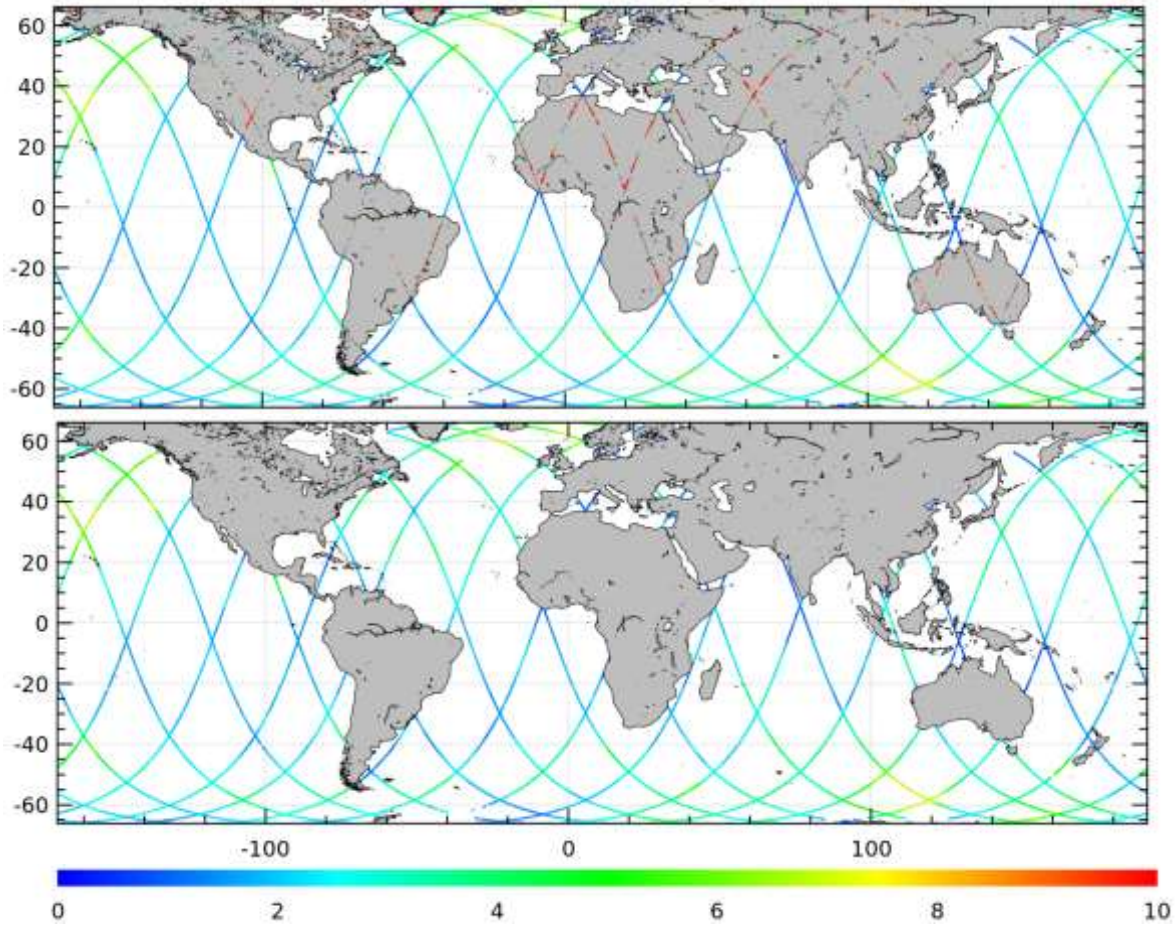

Figure 25: Jason-3 along-track significant wave height measurements on the 14th of January 2018 (cycle 71, tracks 64 to 89) before (top) and after editing (bottom).

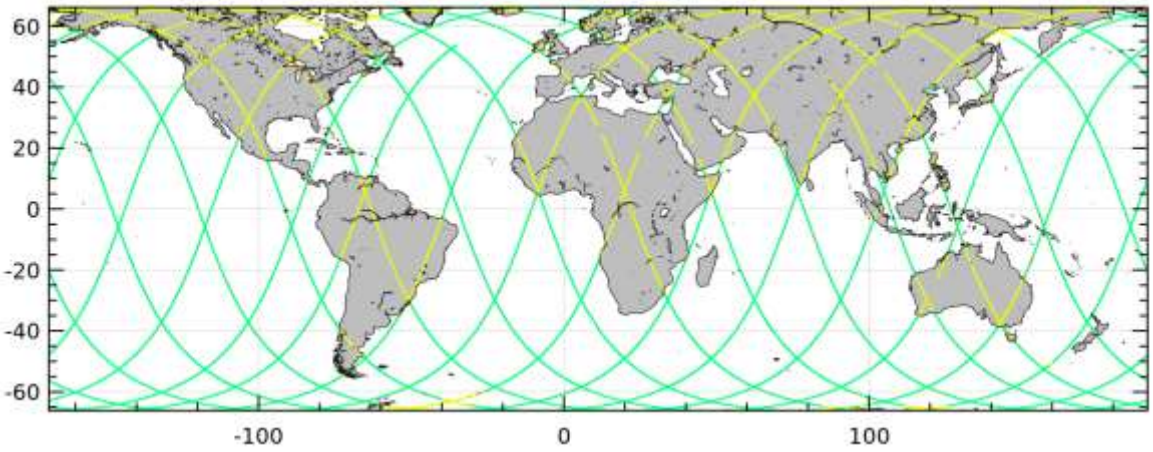

Figure 26: Flags used for the editing of Jason-3 along-track significant wave height measurements on the 14th of January 2018 (cycle 71, tracks 64 to 89). Green = valid, yellow = rejected by ice and surface type flags, red= rejected by threshold criteria.

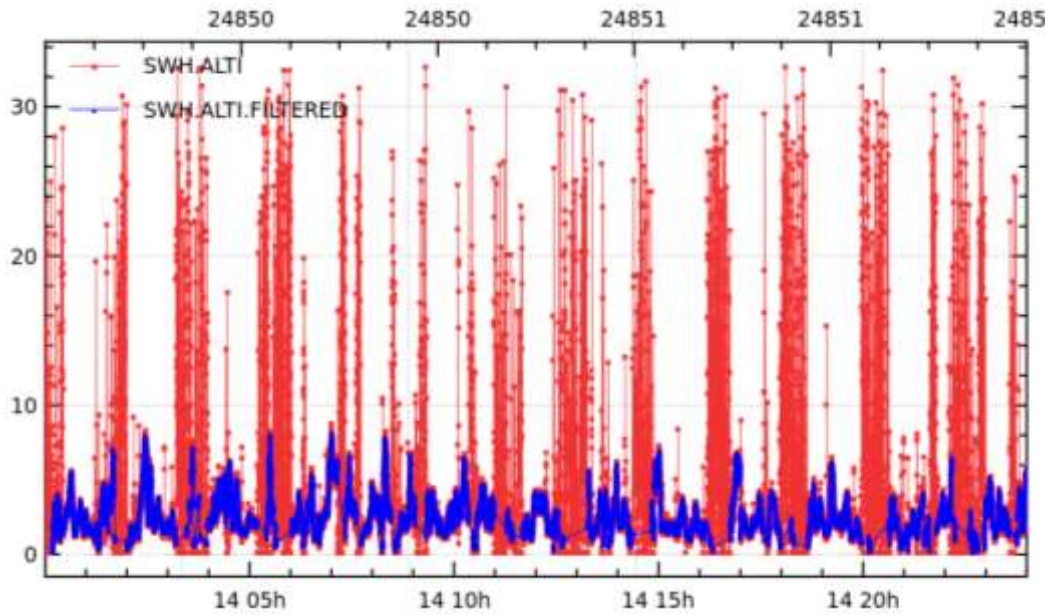

Figure 27: Timeseries of Jason-3 along-track significant wave height measurements on the 14th of January 2018 (cycle 71, tracks 64 to 89) before (red) and after editing (blue).

We finally compared the statistics of rejected measurements to the sea level editing approach at Jason-3 and Sentinel-3A 3-hour crossovers. Results are similar in terms of significant wave height dispersion between the two missions but allows having about 6% more points due to the relaxed constraints on geophysical parameters in the wave editing approach.

VII.1.2 Calibration

Calibration is divided in two main steps (see Figure 28): absolute calibration of a long reference mission against in-situ data and then a cross-calibration of all other satellites with the reference mission.

The first step consists in applying a correction computed between the reference mission and in-situ measurements provided by buoys.

The second step involves homogenising the data from the different missions. Significant wave height measurements from each mission are calibrated against those of a reference mission.

Finally, another calibration step can be added to the process when upstream L2 products evolve for a mission already implemented in the L2P alti wave chain (see Figure 28, L2 version upgrade in yellow). A new calibration for the physical variables of interest is determined between the current and the upcoming L2 versions and is added to the existing calibration of this mission in the L2P alti wave chain.

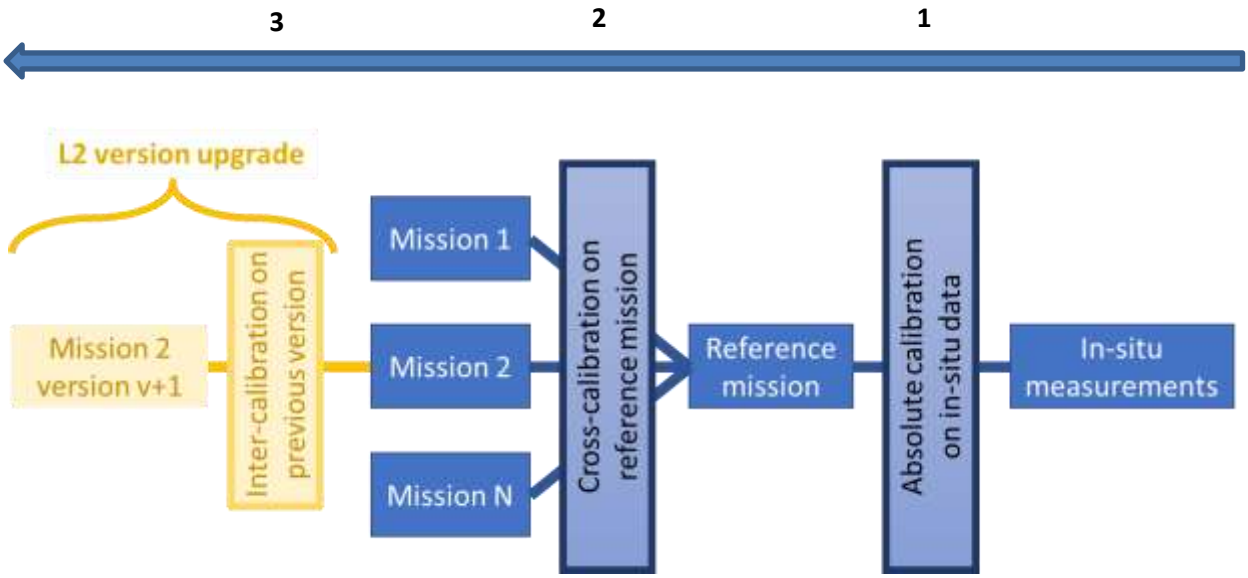

Figure 28: Description of the calibration process.

The following sub-sections describe the computation of the two main calibrations: absolute calibration and cross-calibration.

VII.1.2.1 Significant wave height absolute calibration with regard to in situ

The absolute calibration corrects the biases between in-situ measurements and satellite altimetry. All the missions are cross-calibrated with the reference mission, i.e. Jason-3—this also goes for Sentinel-6A until such a time as enough data exists to recalibrate Sentinal-6A against in-situ data (regardless of this, missions added after the tandem orbit period of Jason-3 and Sentinel-6A will be cross-calibrated against Sentinal-6A).Therefore, the absolute calibration need only to be computed from a comparison of significant wave heights from Jason-3 with those of buoy measurements at collocated points.

For this version, the absolute calibration has been updated. Whereas before it was based on a linear relation calculated for Jason-2 [Queffeulou and Croizé-Fillon, 2017], now that a sufficiently long record exists for Jason-3, it has been recalculated, and instead of a linear fit it takes the form of a lookup table. This enables the calibration to account for non-linearities in the comparison between the in situ and the altimetric data. The procedure involved binning the in situ–altimeter differences in overlapping bins, and for each of them the median value of the differences was taken. For SWH values between 1.5 m and 6 m a linear regression was calculated, which was extrapolated to SWHs higher than 6 m. Note that below 0.3m the number of matchups was too low to get a robust estimate of the median. (For more information on the calibration, see Dodet and Piollé [2021]). To illustrate the lookup table, it has been *plotted* in Figure 29. *The old linear fit is included for comparison; it takes the form* $\mathrm{H_{corr}} = 1.0149\ \mathrm{H} + 0.0277$.

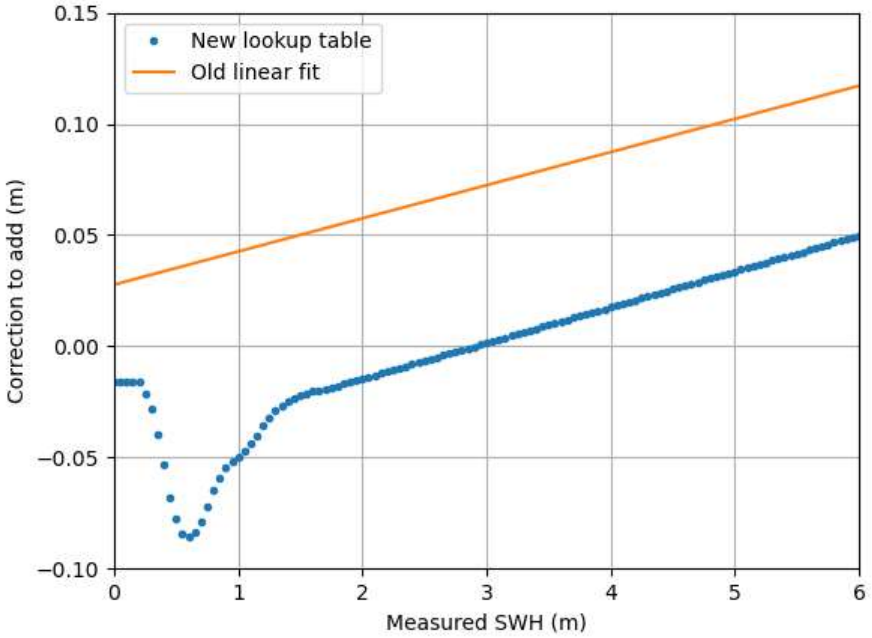

Figure 29 :Graphical illustration of the new lookup table for Jason-3 (blue), with the old linear fit originally calculated for Jason-2 for comparison. For SWHs above 6 m the correction is a linear extrapolation. The corrections are added to the measured SWH.

Another more subtle difference is that the new lookup table is applied only once, to Jason-3. Thereafter the other missions are cross-calibrated with Jason-3. For the previous version, the cross calibration was done first, and the linear absolute calibration was applied to each mission afterwards.

VII.1.2.2 Significant wave height calibration against reference mission

Cross-calibration consists in determining the relation between the significant wave height measurements provided by two different missions. This relation is determined on a representative number of collocated measurements and then used in the operational system to homogenise the missions with respect to the reference one. Such a relation is expected to remain valid as long as instrumental drifts are not detected or ground segment evolutions do not affect the input of L2 products input into the operational system. Should one of these evolve, another cross-calibration relation should be computed and implemented in the operational system.

The reference mission should be a conventional altimeter mission, expected to produce robust SWH measurements.

Two different methods of collocation can be considered, depending on the orbit of the mission to be calibrated with respect to the orbit of the reference mission.

The first one is applied during the “tandem phase”, if it exists, between two missions: both satellites are on the same ground track separated by a few minutes. A very large number of spatially collocated measurements are therefore available for cross-calibration.

The second method is employed when the two missions are on different ground tracks, or no validation phase is available. Crossover points between the two missions are determined. For SWH measurement calibration, only crossover points with a time difference lower than 3 hours are considered. This short delay ensures that both missions observe an ocean state scene that has not significantly evolved (when a longer data record is available, this time difference can be lowered to 1 hour). The 1 Hz along track data for each mission is then interpolated at the selected crossover points using splines. The interpolation technique consists in spline approximation. The procedure relies on an error estimate, and for this the average noise of the SWH measurements is used. This corresponds to the uncertainty in the 1 Hz significant wave height values computed from the high frequency values (20 Hz for most altimeters, Jason-3, Cryosat-2 and Sentinel-3A and 40 Hz for AltiKa).

Once the two missions' measurements are collocated, the differences between the reference mission and the secondary mission's significant wave heights are computed. The bias is plotted as a function of the secondary mission's wave height in order to provide a height-dependent bias correction. The next step is to fit a polynomial function to the distribution of this bias. This function is finally inserted in the L2P alti wave chain to be systematically applied to all L2 valid measurements of the secondary mission.

The following sub-sections present the computation of the cross-calibration between the secondary missions and the reference mission. Some tests on cross-calibration uncertainties are presented in Section IV.3.1.

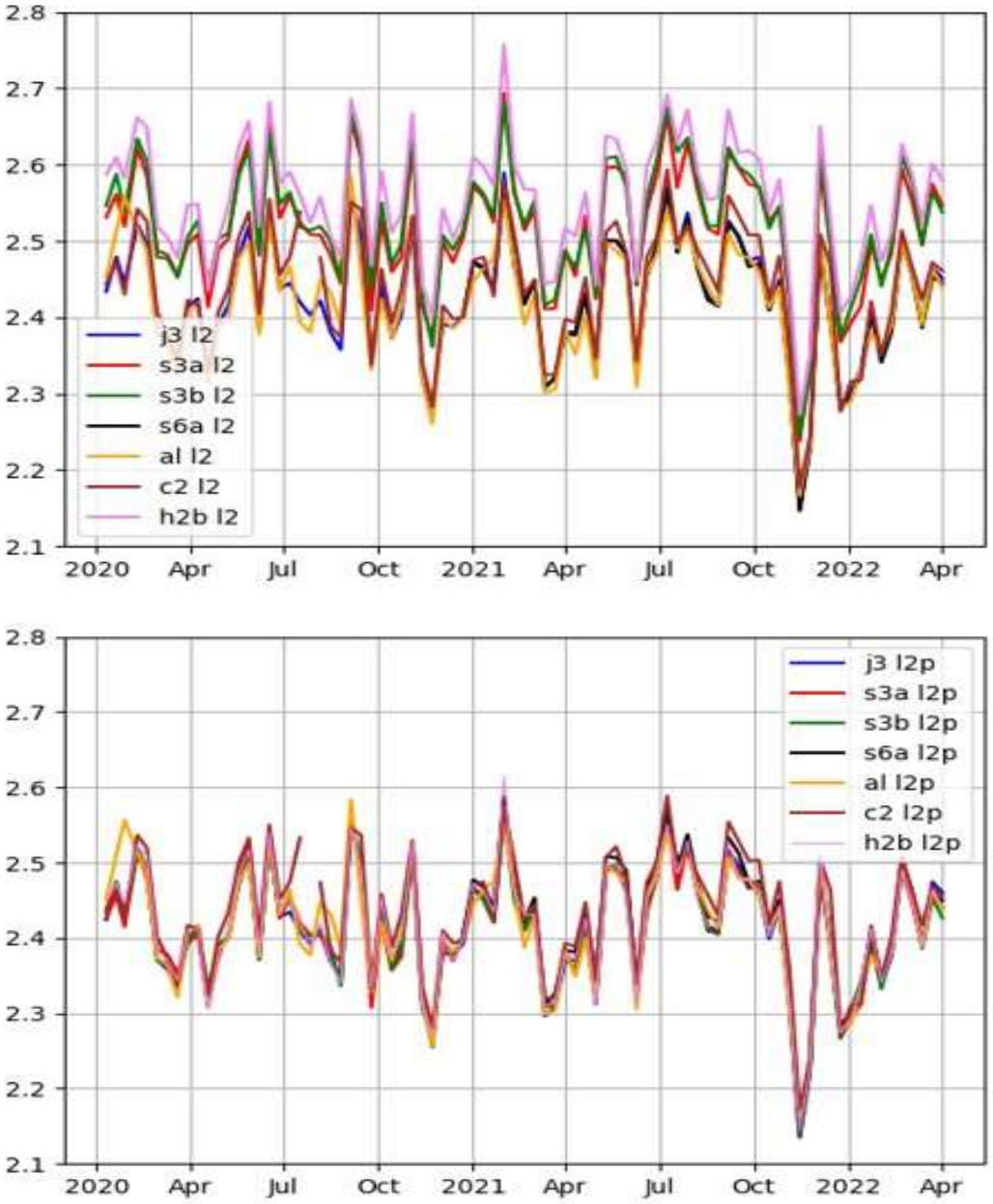

Figure 30: SWH 10-day global weighted mean (m) for L2 (top) dataset and L2P calibrated (bottom) dataset for each mission. The same global weighted mean method as for Global Mean Sea Level (GMSL) is used to have a homogeneous geographical data repartition to compare all mission together.

Figure 30 shows how L2P calibration reduces the differences between each mission from a global mean of more than 10 cm to less than 2 cm (i.e., not only over crossover points). The SWH estimated from all the missions, before and after calibration, were also compared to the SWH from ERA5 model, see Figure 31. There is a better correlation between ERA5 model and L2P (after calibration, bottom plot in Figure 31) than between ERA5 model and L2 (before calibration, upper plot in Figure 31).

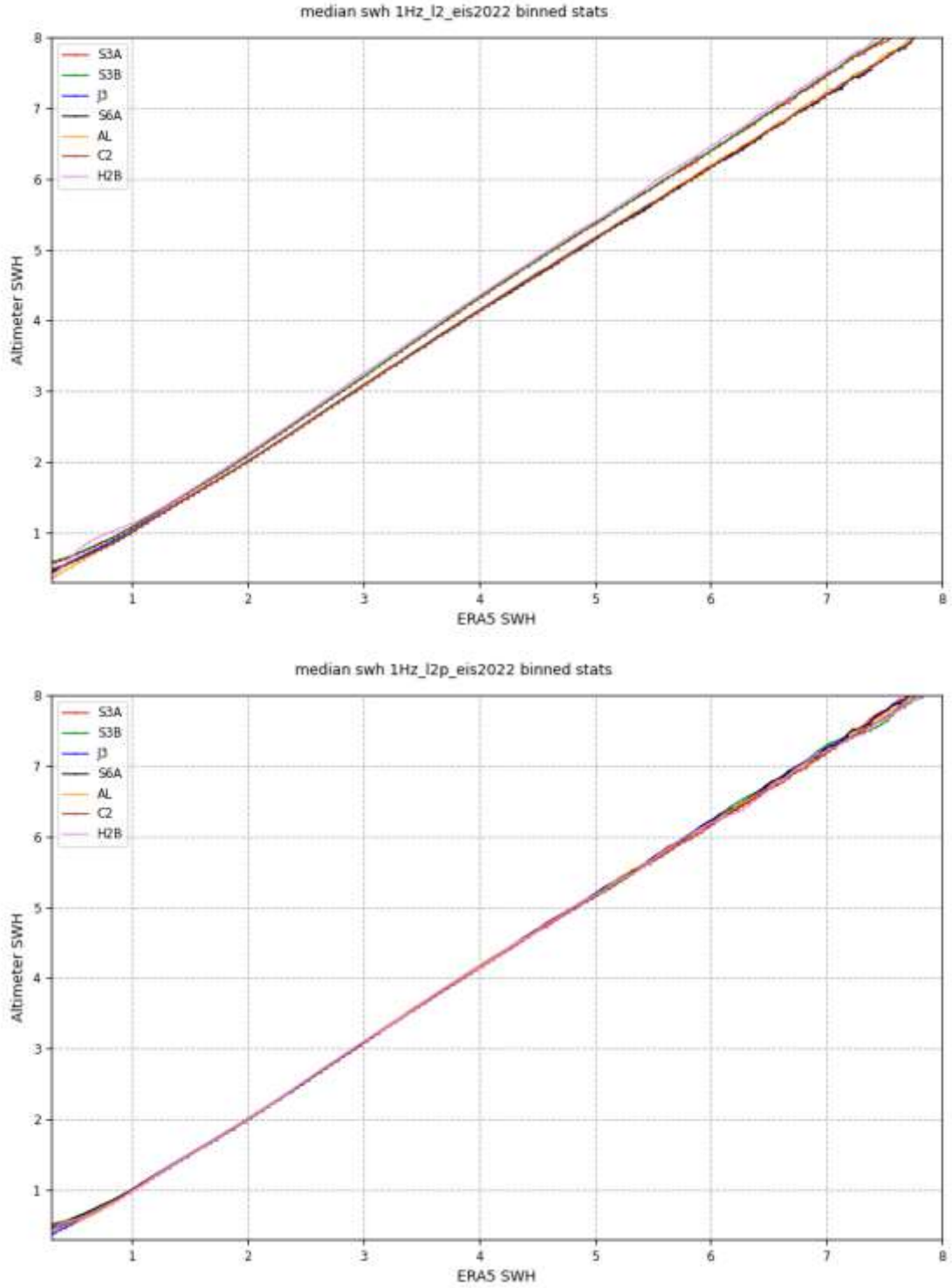

Figure 31: SWH binned of each mission compared to ERA5 model for L2 (top) dataset and L2P calibrated (bottom) dataset. There is a better correlation between ERA5 and all satellite over SWH after L2P calibration. Waves under 0.3m are not shown as the population is too small to be representative of the median.

VII.1.2.2.1 Reference mission change

Jason-3 is the reference mission until April 2022. Then, Sentinel-6A has become the reference mission. However, the calculation of the absolute calibration with in situ data requires a long record of stable measurements (around 3-4 years) to be robust so at present the lookup table defined for Jason-3 will be used for Sentinel-6A. Sentinel-6A was calibrated against Jason-3 (itself calibrated against in-situ data) during the tandem phase, allowing a robust assessment of the biases between the two missions (each S6A measurement is collocated with a J3 measurement).

Sentinel-6A and Jason-3 were cross-calibrated during the tandem phase. The period used to compute the cross-calibration is from 21/09/2021 to 07/04/2022, corresponding to Sentinel-6A's side B data tandem phase with Jason 3.

The significant wave height differences between Sentinel-6A and Jason-3 are represented as a function of Sentinel-6A SWH values in Figure 32. During the tandem phase, the two satellites are acquiring data using the same ground track separated by a few seconds. The number of points used for the cross-calibration is maximal and the time difference between two measurements is extremely small (few seconds). This allows an optimal calculation of the bias correction. The fitting curve is stored in an abacus to be used in the processing chain.

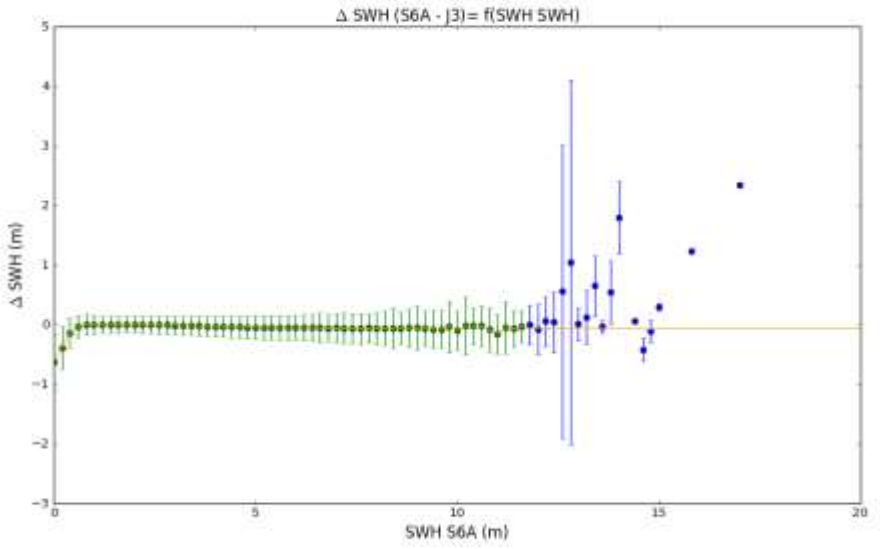

Figure 32: SWH difference between Sentinel-6A L2 and Jason-3 L2P as a function of SWH, divided in 10-cm bins, calculated during the tandem phase. Error bars represent the standard deviation of the difference inside each bin. The yellow curve represents the fitting formula.

Since April 2022, Sentinel-6A has become the reference mission. It is now the reference for bias monitoring at crossovers with other missions and the reference for the calculation of cross-calibration of future missions to be integrated in the system.

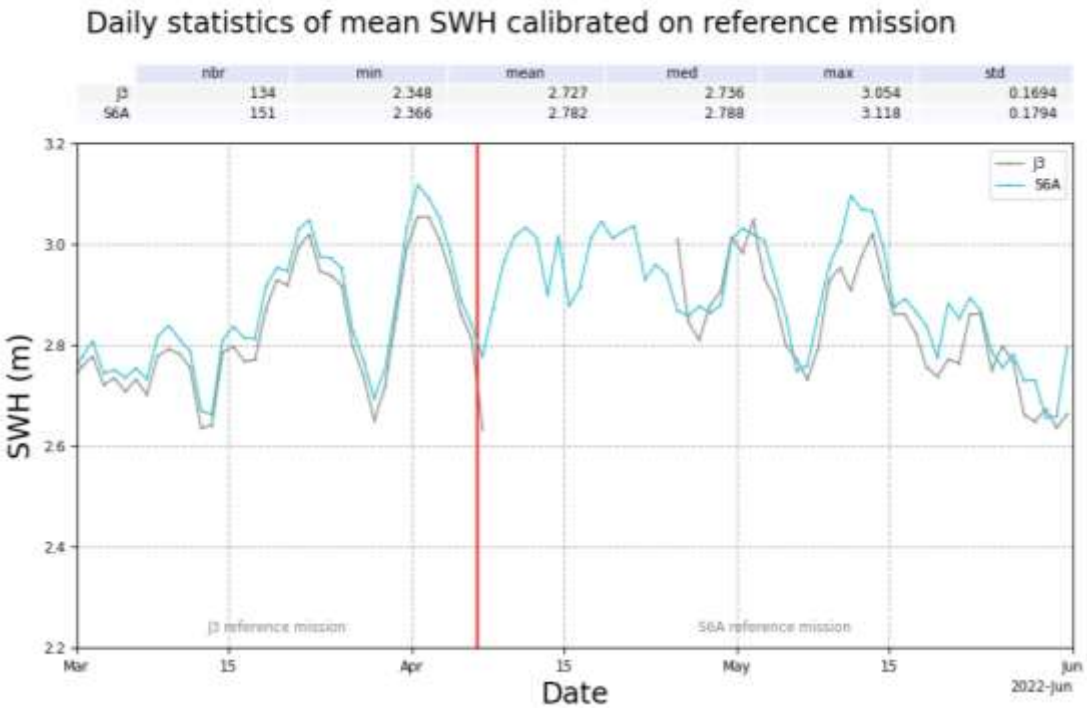

Figure 33: Daily statistics of mean SWH calibrated on reference missions. Sentinel 6A is calibrated over Jason 3 during the tandem phase, then Jason 3 moves from its orbit to an interleaved orbit between 2 tracks.

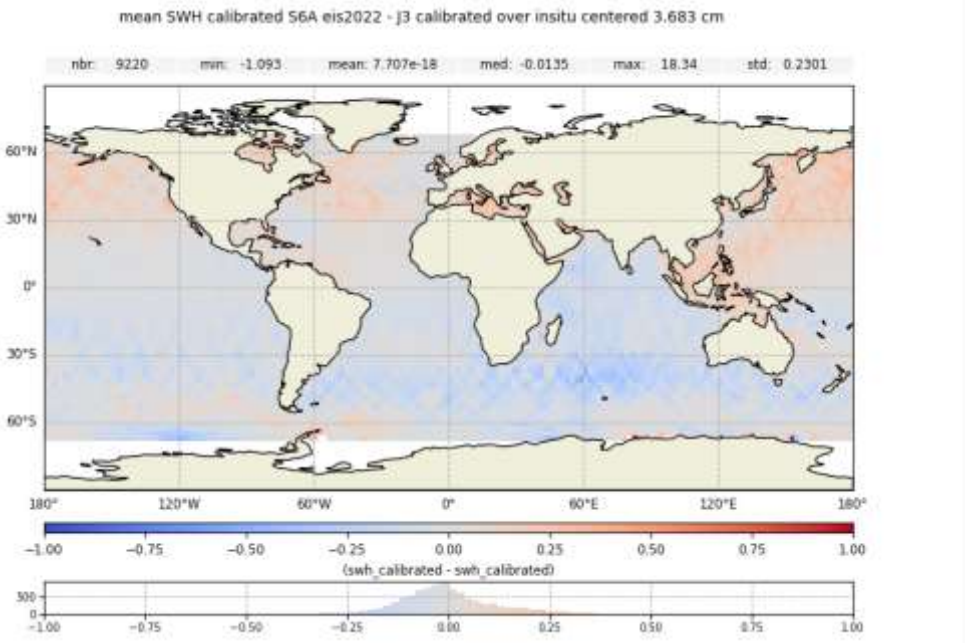

Figure 34: SWH residual differences between Sentinel 6A calibrated over J3 against J3 calibrated over in situ during the tandem phase

Figure 34 and Figure 35 show good agreement between Jason 3 and Sentinel 6A even after Jason 3 orbit change. Nord/South differences are observed.

VII.1.2.3 Calibration performance

To verify the performance of the new calibration, an independent data set was needed. For the calibration, Dodet and Piollé (2022) used the reprocessed in situ data set INSITU_GLO_WAVE_REP_OBSERVATIONS_013_045[1] from the Copernicus Marine Service In Situ Thematic Assembly Centre (INSTAC)[2], and the same data source was used for validation. Since as many in situ platforms as possible that fit the quality requirements (Dodet and Piollé, 2022) were used to generate the lookup table, it was not possible to find a set of independent platforms, so independence here is limited to the temporal window. The calibration used data from 17th February 2017 to 13th June 2021; thus, data from 14th June 2021 could be used for the validation. The period of time of data used for validation was from 14th June 2021 to 4th April 2022. Sentinel-6A is a special case as its entry into service was much later in 2021, although it was in orbit long before that date. For the retreatment, data prior to its entry into service is included, but because this is absent from the previous production, a before-and-after comparison cannot be made over the same period as the other missions. There are therefore two separate validations for Sentinel-6A: a comparison over a reduced period, from 25th November 2021 to 4th April 2022, of the old and new calibrations, and a validation over the full period of 14th June 2021 to 4th April 2022 of Sentinal-6A with the new calibration only, so that it can be compared with Jason 3.

The validation procedure implemented here matches altimetric observations to hourly in situ data within a time window of 30 minutes and a distance of 50 km. The in situ data are quired to be at least 100 km from the coast, which also guarantees that the altimetric data are at least 50 km from the coast, which helps avoid problems with incompatible SWH measurements (for example a buoy measurement in open ocean compared with an altimetric SWH where the wave state is modified by coastal processes). The collocated altimetric data is averaged to produce a mean SWH to match a single in situ observation.

Statistics for the validation period are summarised in Table 15 for both the old and new calibrations, for each mission independently. The statistical quantities used are defined as follows:

The root mean squared error (RMSD) is defined as

$$RMSD = \sqrt{\frac{1}{N}\sum_{i=1}^{N}(a_i - b_i)^2} \qquad \text{(Eq. 1)}$$

the scatter index (SI) is defined as

$$SI = \sqrt{\frac{\sum_{i=1}^{N}(a_i - \bar{a} - b_i + \bar{b})^2}{\sum_{i=1}^{N} {b_i}^2}} \qquad \text{(Eq. 2)}$$

and the Hanna and Heinold indicator (HH, Hanna and Heinold, 1985) is defined as

$$HH = \sqrt{\frac{\sum_{i=1}^{N}(a_i - b_i)^2}{\sum_{i=1}^{N} a_i b_i}} \qquad \text{(Eq. 3)}$$

where a_i and b_i are the ith colocalised altimetric and in situ observations, respectively, and the overbars represent the mean over all *N* colocalisations.

The new calibration produces a lower bias for every mission, and a lower RMSE. Sometimes the scatter index is higher with the new calibration, however it has been noted that this measure (and the RMSE) is

[1] https://data.marine.copernicus.eu/product/INSITU_GLO_WAV_DISCRETE_MY_013_045/description [last accessed 5th December 2023]

[2] https://marine.copernicus.eu/about/producers/insitu-tac [last accessed 4th October 2022]

not always reliable, because the mean and scatter are partially linearly dependent (Mentaschi et al., 2013). The HH index is a more reliable indicator for validation purposes (Mentaschi et al, 2013), so it is included here as well, and it unambiguously favours the new calibration over the old one.

Mission/ Calib.	Bias (m)	RMSE (m)	SI %	HH %	R	NbBuoys	Colloc
AL/old	0.096	0.199	7.61	8.58	0.989	45	748
AL/new	0.005	0.175	7.65	7.68	0.989	45	763
C2/old	0.086	0.198	7.87	8.60	0.988	44	764
C2/new	0.027	0.181	7.90	7.97	0.988	45	777
CFO/old	0.109	0.206	7.27	8.46	0.991	44	757
CFO/new	-0.018	0.174	7.19	7.29	0.991	44	777
H2B/old	0.102	0.328	12.69	13.20	0.967	35	640
H2B/new	0.023	0.306	12.42	12.47	0.968	35	671
J3/old	0.091	0.208	7.99	8.78	0.988	33	809
J3/new	0.015	0.188	8.00	8.04	0.988	33	807
S3A/old	0.083	0.222	8.58	9.18	0.986	45	740
S3A/new	-0.002	0.202	8.44	8.48	0.987	45	739
S3B/old	0.083	0.213	8.16	8.78	0.987	45	809
S3B/new	0.008	0.195	8.06	8.09	0.988	45	801
S6A/old*	0.072*	0.233*	7.84*	8.21*	0.988*	29*	373*
S6A/new*	0.004*	0.221*	7.84*	7.89*	0.988*	29*	373*
S6A/new	0.021	0.191	8.02	8.08	0.987	34	792
H2C	0.014	0.191	8.29	8.33	0.987	33	940
SWOT Nadir	0.046	0.168	9.93	10.21	0.977	38	124

*Table 15: Validation statistics against in situ data for each mission. Statistics for the "old" (linear fit) absolute calibration are given followed immediately by those for the "new" calibration (implemented as a lookup table) in the present release. *For Sentinal-6A, these rows were calculated over a shorter period corresponding to the service period for that mission. The retreatment with the new calibration used data prior to the entry into service and this is presented in the unstarred row. † Preliminary data for SWOT nadir is used over a different period – it is to be understood as indicative only. A proper validation of SWOT Nadir will be undertaken after its entry into service.*

VII.1.2.4 Wind speed cross-calibration

As for significant wave height, wind speed cross-calibration consists in determining the relation between the wind speed measurements provided by two different missions. This relation is determined on a representative number of collocated measurements and then used in the operational system to homogenise the missions with respect to the reference one, here Jason 3 (until April 2022). The relation is expected to remain valid as long as no instrumental drifts are detected, or ground segment evolutions are implemented over Level 2 production. Should one of these evolve, another cross-calibration relation should be computed and implemented into the operational system.

As explained earlier (section IV.1.2), the second method of cross-calibration is the one used in the following as all of the considered mission have a different orbit from Jason3. For wind speed calibration, only crossover points with a time difference lower than 3 hours are considered (when a longer dataset is available, this time difference can be lowered down to 1 hour). The 1 Hz along track data for each mission is then interpolated at the selected crossover points. The interpolation technique consists in an along-track spline interpolation of wind speed values at the crossover location. Once the two missions' measurements are collocated, the differences between the reference mission and the secondary mission are computed. The bias is plotted as a function of the secondary mission wind speed in order to provide a wind-dependent bias correction. The next step consists in fitting a polynomial function to the distribution of this bias. This function is finally inserted in the L2P alti wave chain to be systematically applied to all L2 valid measurements of the secondary mission.

The following sub-sections present the computation of the cross-calibration between the secondary missions and the reference mission.

VII.1.2.4.1 Sentinel-3A SAR wind speed calibration

The same principle as for SWH is used for wind speed calibration. Sentinel-3A crossover points with Jason-3 were computed over a 117-day period (January 22nd, 2020, to May 18th, 2020). The starting date corresponds to the new version of Sentinel-3A L2 NRT production with the Samosa 2.5 ocean retracker to determine the backscatter coefficient used in the wind computation (Abdallah 2007). Figure 35 presents the spatial distribution of the valid crossover points (after the editing process). Figure 32 shows the representativeness of wind values at crossover points with respect to the valid along-track values over the same period. The distribution within crossover points is skewed towards larger wind speed values due to the higher density of crossover points at high latitudes, where the mean wind speed is larger than between inter-tropical bands. Despite these differences, crossover points correctly sample all ranges of wind speed from 2 to 16 m. Outside this interval, the population in each bin of 0.3 m/s (~1 km/h) width is smaller than 30 crossover points and the bin statistic is less reliable for the polynomial fit computation. Hence, bins with less than 30 crossovers are not used for the polynomial fit as shown in Figure 37. Given the piece wise linear shape of the wind-dependency, a smoothed spline interpolation is used for the polynomial fit where the standard deviation (per bin) is used to weight each bin. The polynomial fit is then provided as a table of wind speed calibration biases for S3-B wind speed values ranging from 0m/s to 30m/s with a step of 0.15 m/s.

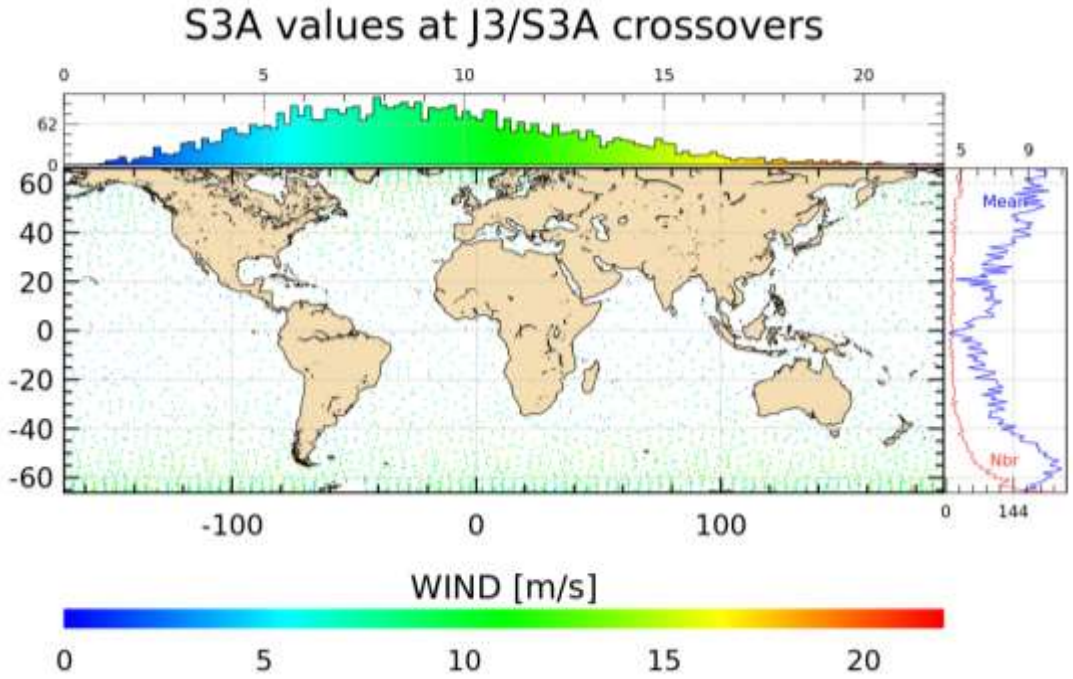

Figure 35: Spatial distribution of S3-A and J3 crossover points. Only valid wind speed values are displayed. Top: histogram of wind values over crossover points. Right: Number of points and mean wind speed valid values as a function of latitude.

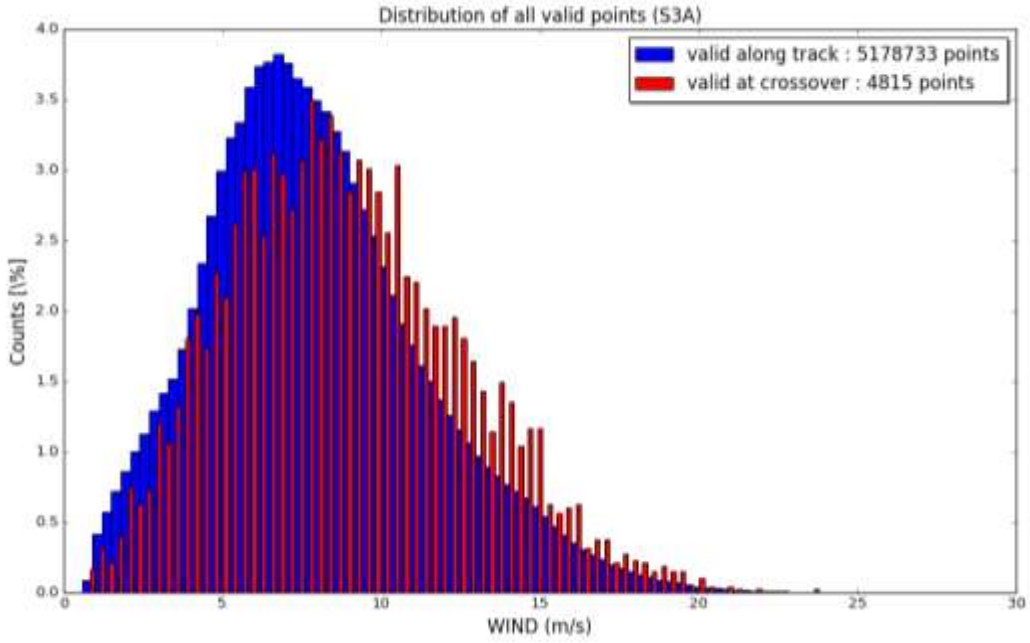

Figure 36: Valid S3-A SAR wind speed distribution over the cross-calibration period with J3.

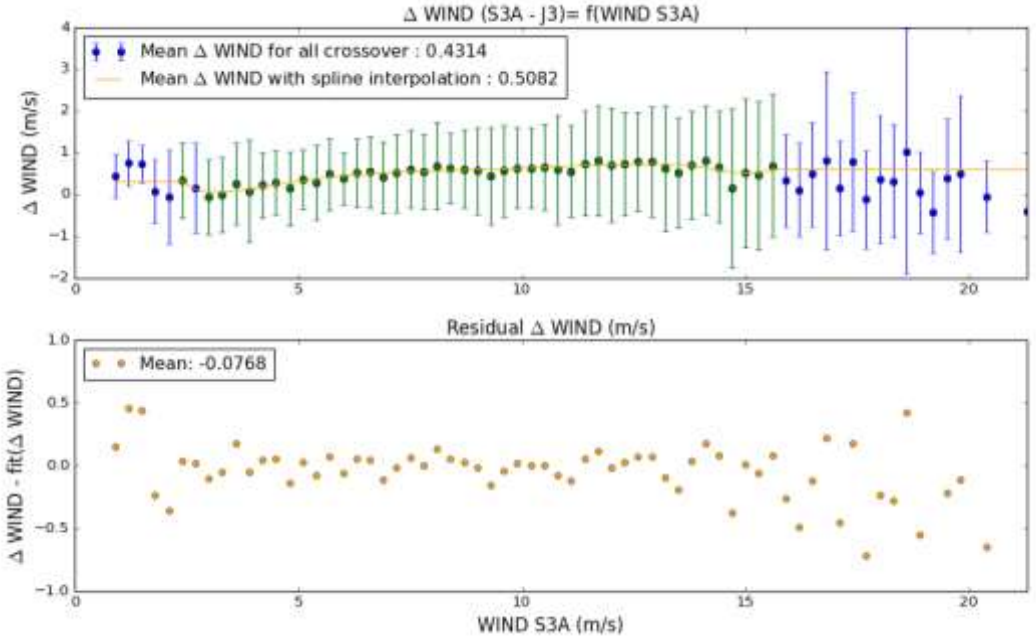

Figure 37: Top: Mean difference between S3-A SAR wind speed values and J3 values per 0.3 m/s (~1 km/h) bin. Error bars represent the standard deviation of the difference inside each bin. Green points in the top panel are the ones selected for the polynomial fit (with more than 30 crossover points) represented by the orange curve. Bottom: the residual difference between the value per bin and the fit.

VII.1.2.4.2 Sentinel-3B wind speed calibration

A direct cross-calibration method is used to compute Sentinel-3B wind calibration speed, over the same period as Sentinel-3A (January 22nd, 2020, to May 18th, 2020). Figure 38 presents the spatial distribution of the valid crossover points and Figure 39 shows the representativeness of wind values at crossover points with respect to the valid along-track values. For the same reasons as for S3A (section VII.1.2.4.1) the distribution within crossover points is skewed towards larger wind speed values, and bins with less than 30 crossovers are not used for the polynomial fit as shown on Figure 40 . The polynomial fit is then provided as a table of wind speed calibration biases for S3-B wind speed values ranging for 0 m/s to 30 m/s with a step of 0.15 m/s (500 m/h).

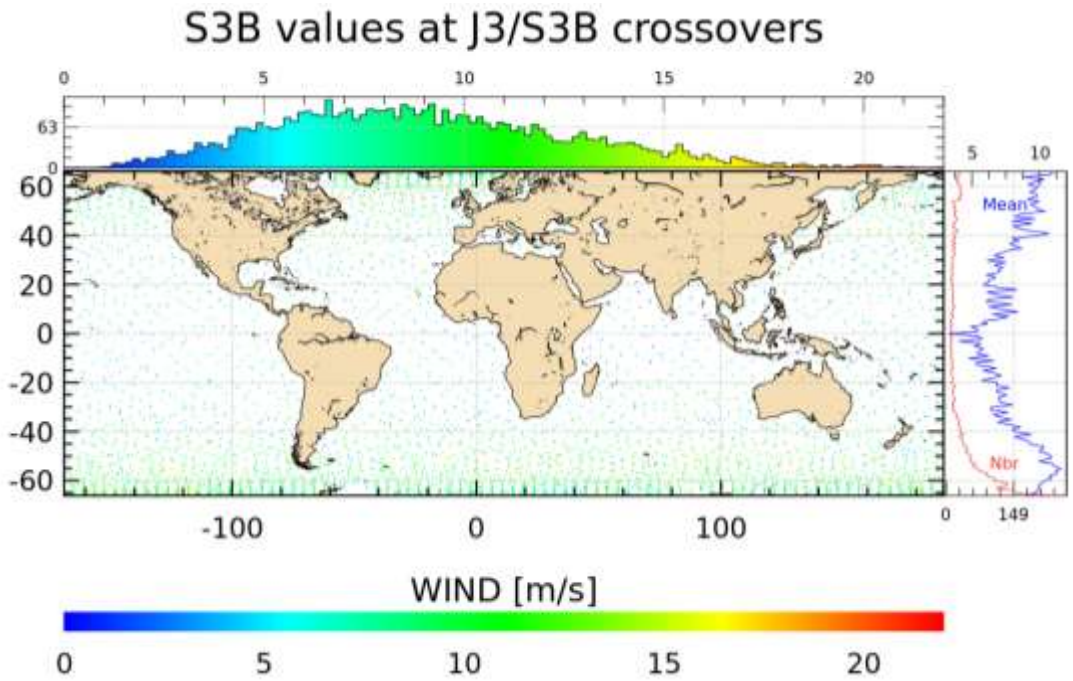

Figure 38 : Spatial distribution of S3-B SAR and J-3 crossover points. Only valid wind values are displayed. Top: histogram of wind values over crossover points. Right: Number of points and mean wind speed valid values as a function of latitude.

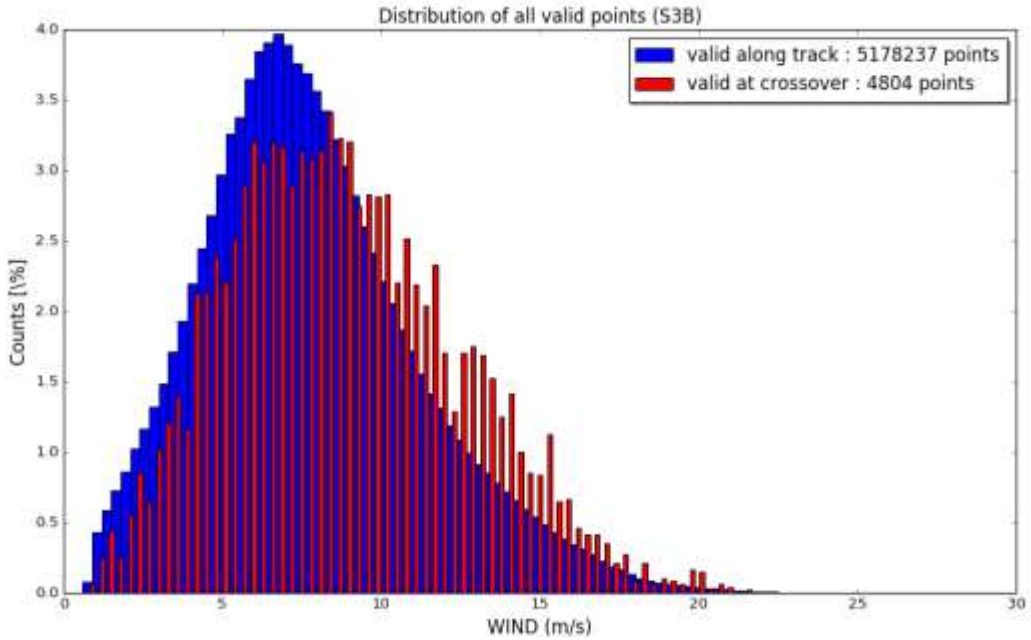

Figure 39 : Valid S3-B SAR wind speed distribution over the cross-calibration period with J3.

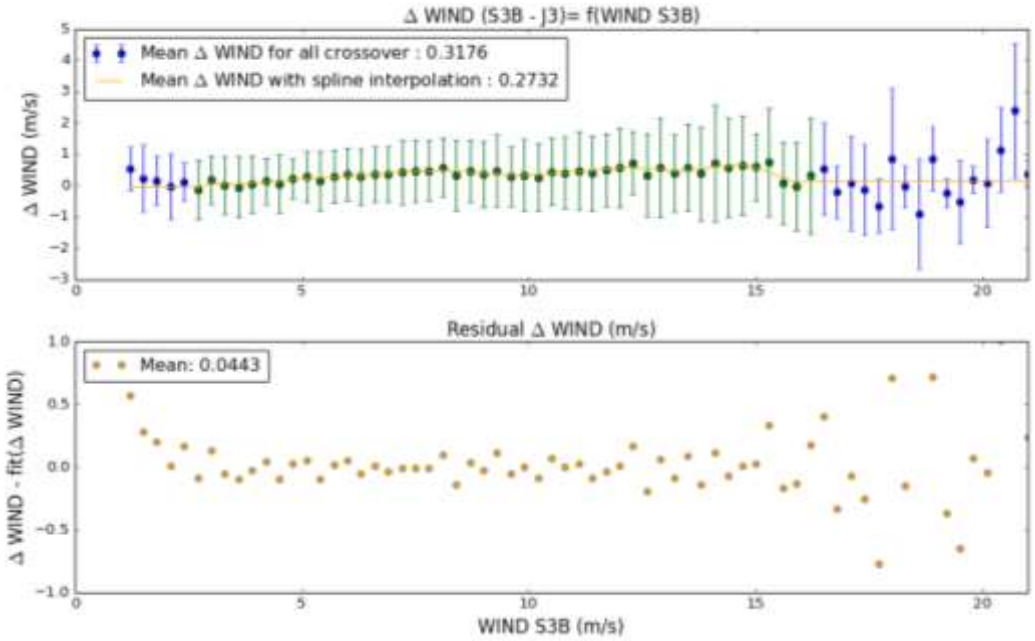

Figure 40 : Top: Mean difference between S3-B SAR wind speed values and J3 values per 0.3 m/s (~1 km/h) bin. Error bars represent the standard deviation of the difference inside each bin. Green points on the top panel are the one selected for the polynomial fit (with more than 30 crossover points) represented by the orange curve. Bottom, the residual difference between the value per bin and the fit.

VII.1.2.4.3 SARAL/AltiKa wind speed calibration

Calibration of SARAL/AltiKa's wind speed with Jason-3 was also performed using the crossover method with a time difference lower than 3 hours. SARAL / Jason-3 crossover differences were computed over an 81-day period (February 27th, 2020, to May 18th, 2020). The starting date corresponds to the new GDR-F version of SARAL's L2 NRT production using the Tran (2014) table for wind computation. Once the full GDR-F reprocessing is done, the cross-calibration will be recomputed over a 1-year period to have a larger sample of wind speed values. This future calibration will be implemented in the next version of products planned for 2021. The spatial distribution of valid crossovers is presented on Figure 41 . Similarly, the number of crossover points is larger at high latitudes therefore sampling a higher wind speed population. As a result, the distribution of the wind speed values at crossover points is slightly skewed towards larger values when compared to along-track population (Figure 42). Crossover point distribution samples nevertheless all ranges of wind values from 2 to 16 m. The blue dots in Figure 43 represent the mean difference between SARAL and Jason-3 wind speed values for 0.3 m/s bins of the SARAL population, and the bars the standard deviation per bin. As for Sentinel missions, a smoothed spline fit is performed to determine the bias as a function of wind speed values. The polynomial fit is then provided as a table of wind speed calibration biases for SARAL wind speed values ranging for 0 m/s to 30 m/s with a step of 0.15 m/s (500 m/h).

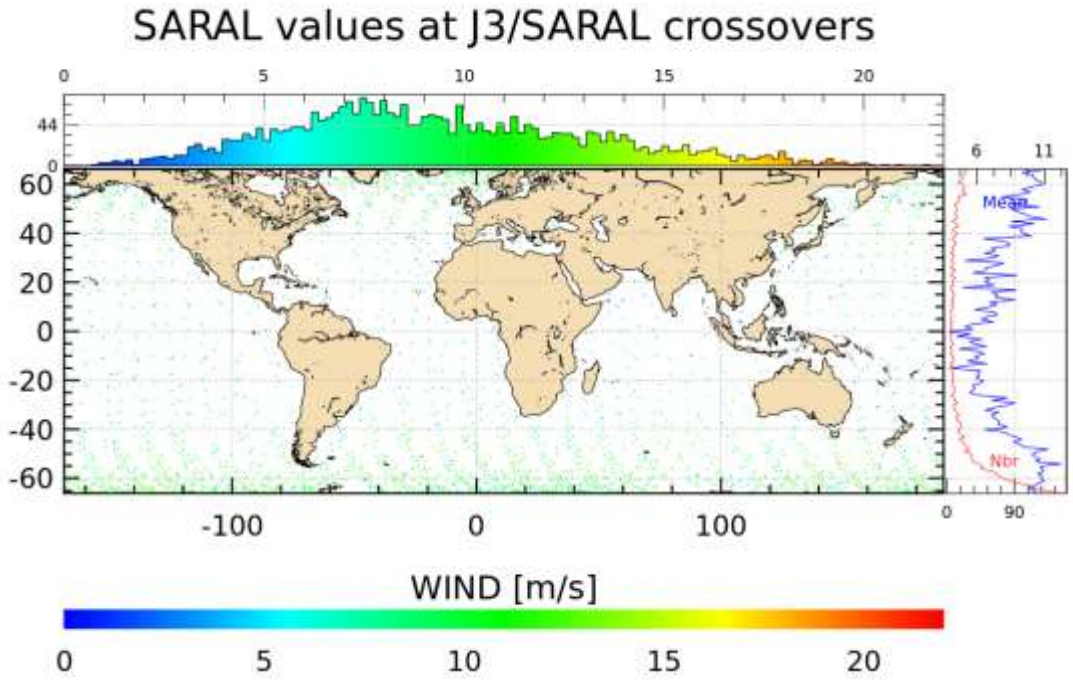

Figure 41 : Spatial distribution of SARAL and Jason-3 crossover points. Only valid wind values are displayed. Top: histogram of wind speed values over crossover points. Right: Number of points and mean wind speed valid values as a function of latitude.

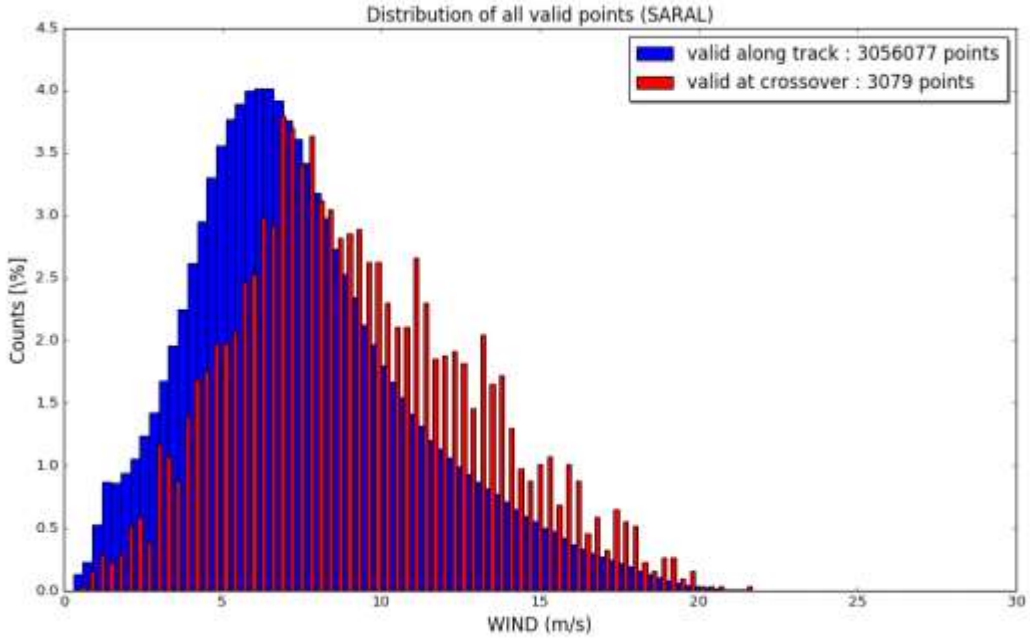

Figure 42 : Valid SARAL wind speed distribution over the cross-calibration period with J3.

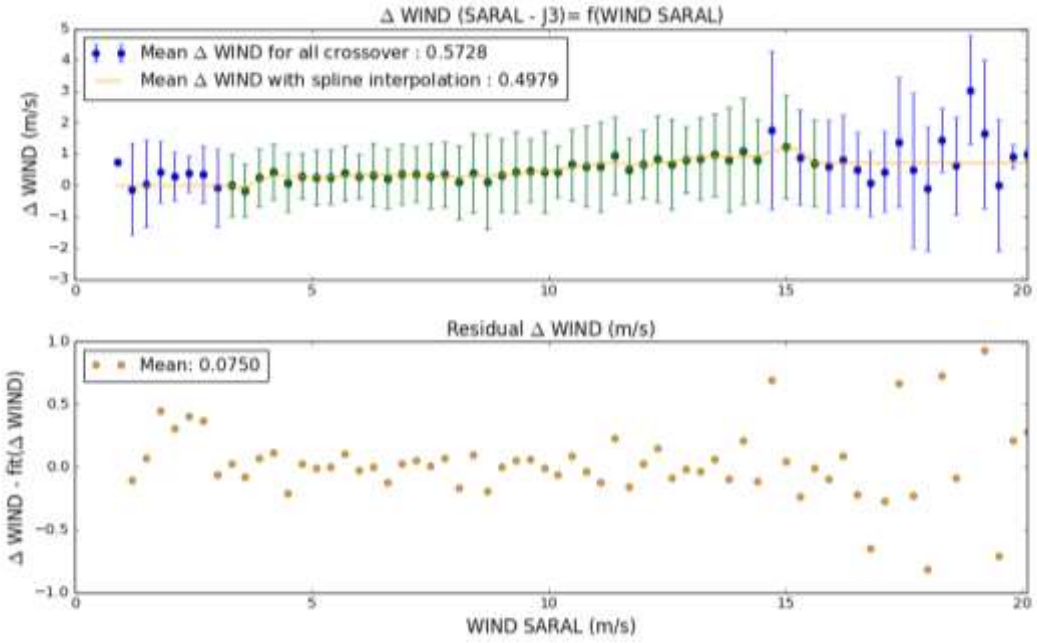

Figure 43 : Top: Mean difference between SARAL wind speed values and J3 values per 0.3 m/s (~1 km/h) bin. Error bars represent the standard deviation of the difference inside each bin. Green points on the top panel are the one selected for the polynomial fit (with more than 30 crossover points) represented by the orange curve. Bottom, the residual difference between the value per bin and the fit.

VII.1.2.4.4 Cryosat-2 wind speed calibration

Calibration of Cryosat-2 wind speed with Jason-3 was performed using the main field of wind speed provided in the baseline C Level 2 product, merging both SAR and LRM measurements. Cryosat-2 / Jason-3 crossover differences were computed over a 366-day period (May 18th, 2019, to May 18th, 2020) allowing to have a greater number of crossovers and to better sample the range of wind speed values. The spatial distribution of valid crossovers is presented on Figure 44 . The distribution of the wind speed values at crossover points is less skewed towards larger values when compared to Sentinel missions or SARAL. It is mainly due to the higher crossover population with middle-ranged wind speeds between intertropical bands that is better sampled given the longer period used for the calibration. Figure 45 shows indeed a crossover point distribution closer to the along-track one that samples all ranges of wind values from 2 to 16 m.

The blue dots in Figure 44 (top) represent the mean difference between Cryosat-2 and Jason-3 wind speed values inside each 0.3 m/s (~1 km/h) bin of the C2 wind speed population. The spline fit is performed with bins containing more than 30 crossovers to determine the bias as a function of wind speed values. The polynomial fit is then provided as a table of wind speed calibration biases for C2 wind speed values ranging for 0 m/s to 30 m/s with a step of 0.15 m/s (500 m/h).

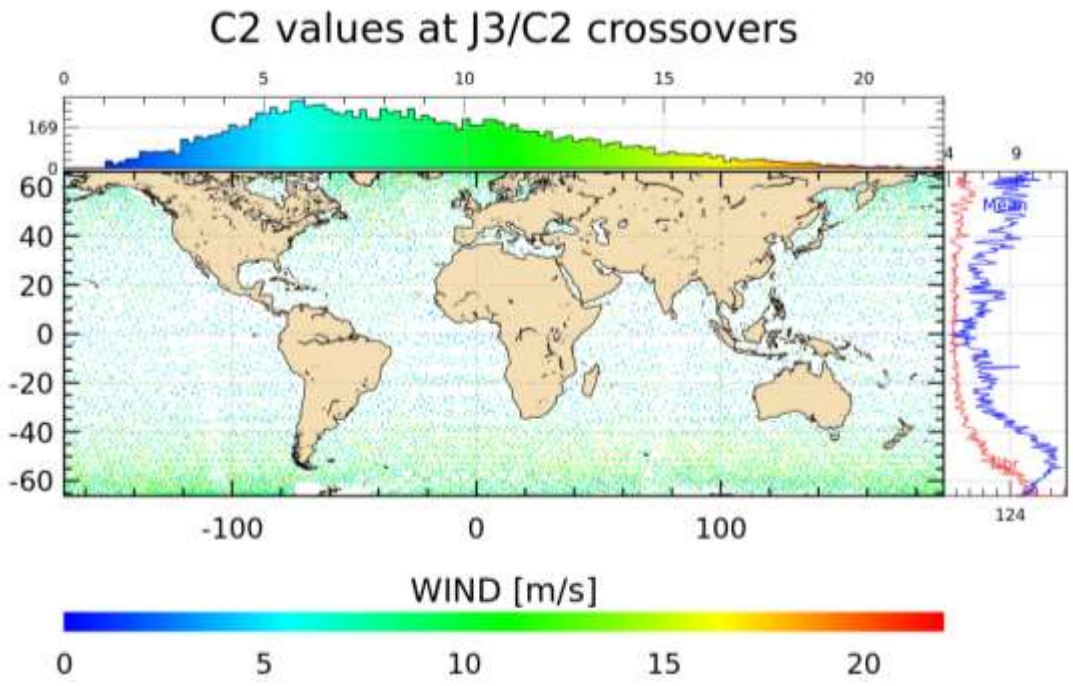

Figure 44 Spatial distribution of Cryosat-2 and Jason-3 crossover points. Only valid wind values are displayed. Top: histogram of wind speed values over crossover points. Right: Number of points and mean wind speed valid values as a function of latitude.

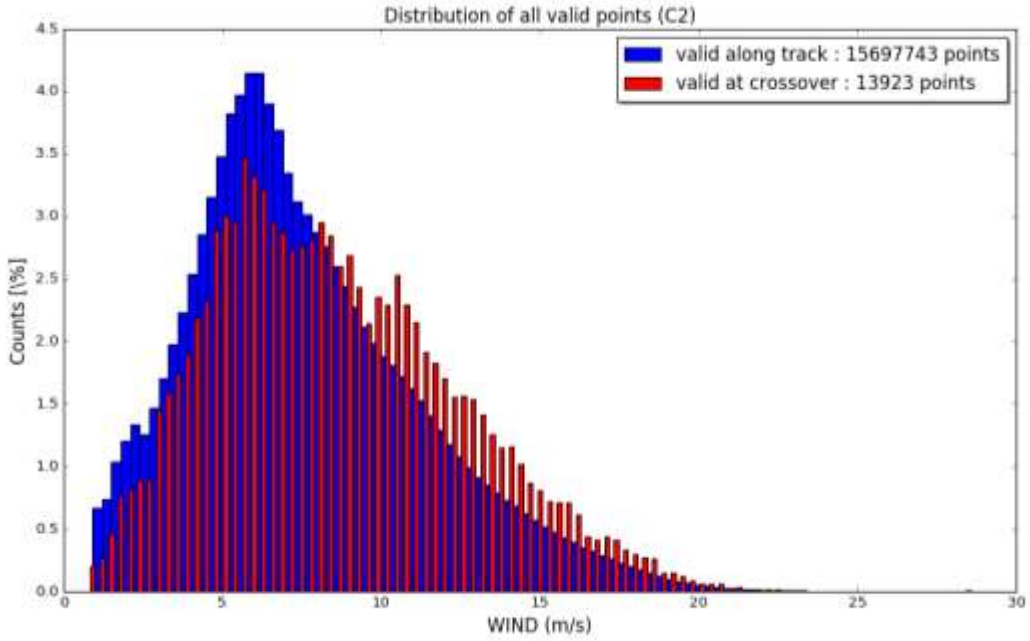

Figure 45: Valid Cryosat wind speed distribution over the cross-calibration period with J3.

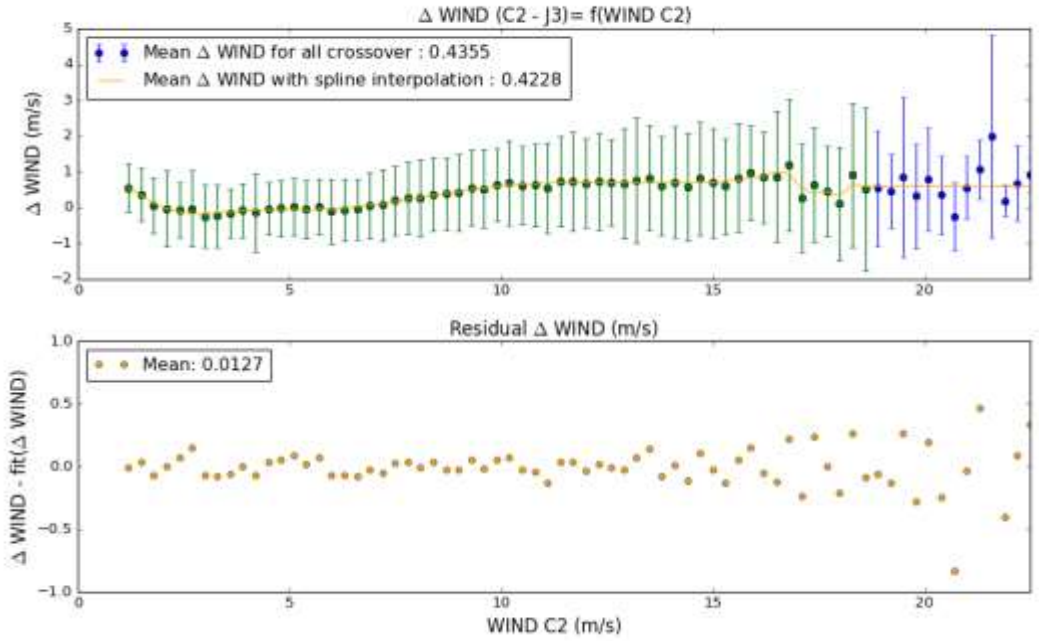

Figure 46 : Top: Mean difference between SARAL wind speed values and J3 values per 0.3 m/s (~1 km/h) bin. Error bars represent the standard deviation of the difference inside each bin. Green points on the top panel are the one selected for the polynomial fit (with more than 30 crossover points) represented by the orange curve. Bottom, the residual difference between the value per bin and the fit.

VII.1.2.4.5 Haiyang-2B wind speed calibration

Calibration of Haiyang-2B (H2B) wind speed with Jason-3 was performed over a 185-day period (November 15th, 2019, to May 18th, 2020). This calibration will be extended to a 1-year period in the next version of L3 products planned for 2021. The spatial distribution of valid crossovers is presented on Figure 47 Figure . The distribution of the wind speed values at crossover points is less skewed towards larger values when compared to Sentinel missions or SARAL. It is mainly due to the higher crossover population with middle-ranged wind speeds between intertropical bands that is better sampled. Figure 48 Figure shows a crossover point distribution that samples all ranges of wind values from 2 to 16 m.

The blue dots in the top panel of Figure 49 represent the mean difference between H2B and Jason-3 wind speed values inside each 0.3 m/s (~1 km/h) bin. The spline fit is performed with bins containing more than 30 crossovers (green dot) to determine the bias as a function of wind speed values. The polynomial fit is then provided as a table of wind speed calibration biases for H2B wind speed values ranging for 0 m/s to 30 m/s with a step of 0.15 m/s (500 m/h).

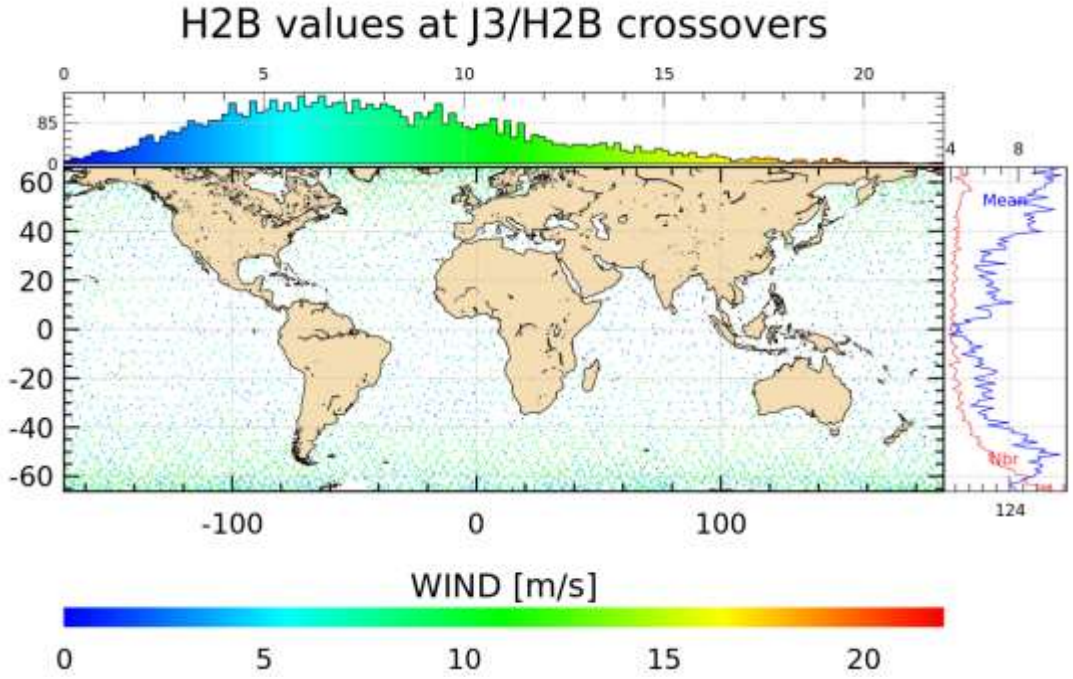

Figure 47 Figure 47: Spatial distribution of H2B and Jason-3 crossover points. Only valid wind values are displayed. Top: histogram of wind speed values over crossover points. Right: Number of points and mean wind speed valid values as a function of latitude.

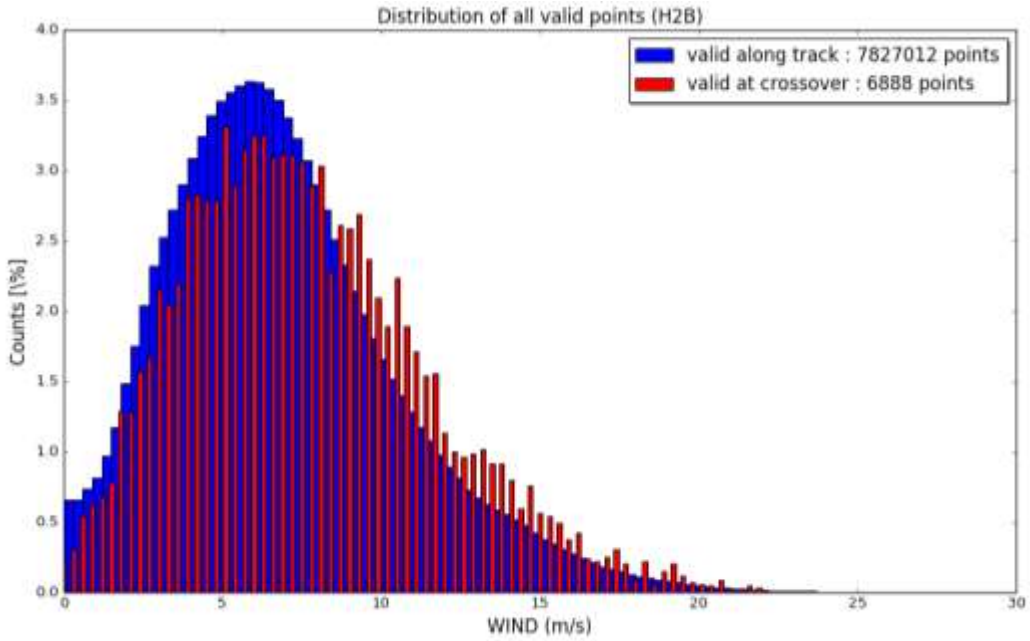

Figure 48 Figure 48: Valid H2B wind speed distribution over the cross-calibration period with J3.

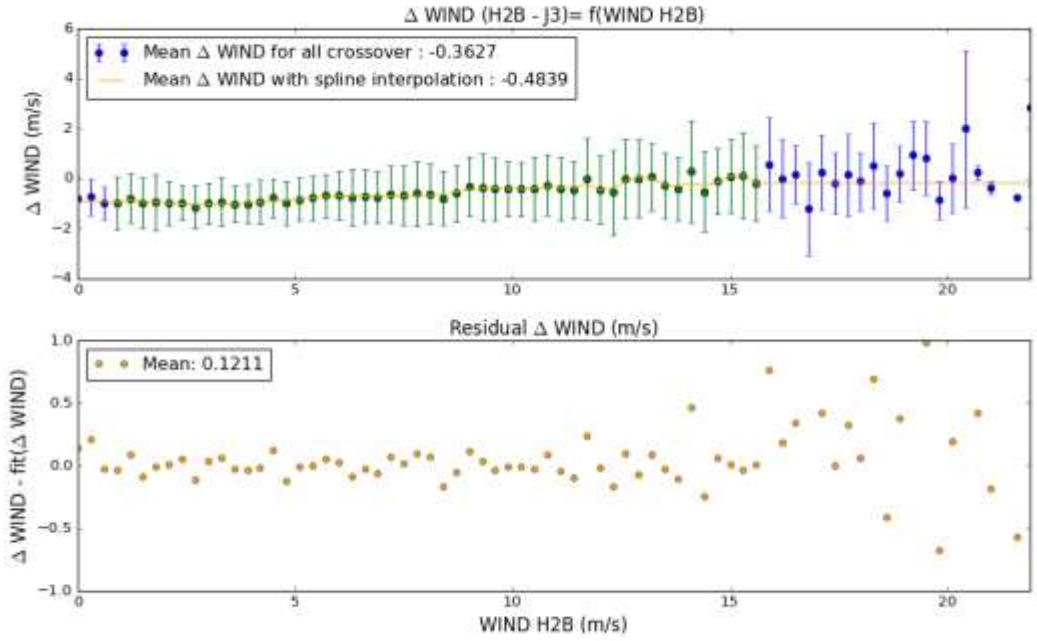

Figure 49: Top: Mean difference between H2B wind speed values and J3 values per 0.3 m/s (~1 km/h) bin. Error bars represent the standard deviation of the difference inside each bin. Green points on the top panel are the one selected for the polynomial fit (with more than 30 crossover points) represented by the orange curve. Bottom, the residual difference between the value per bin and the fit.

VIII REFERENCES

Aviso+, Along-track Level-2+ (L2P) Sentinel-3A Product Handbook, v1.2, 2016d (http://www.aviso.altimetry.fr/fileadmin/documents/data/tools/hdbk_L2P.pdf)

Abdalla, S., 2007: Ku-band radar altimeter surface wind speed algorithm. Proceedings of the Envisat Symposium 2007, H. Lacoste and L. Ouwehand, Eds., European Space Agency Publ. ESA SP636, 463250. [Available online at https://earth.esa.int/workshops/envisatsymposium/proceedings/sessions/3E4/463250sa.pdf.]

Collard, F., 2005: Algorithmes de vent et période moyenne des vagues JASON à base de réseaux de neurones. BO-021-CLS0407-RF, Boost Technologies, 33 pp

Dibarboure, G. et al (2014): Investigating short-wavelength correlared errors on low-resolution mode altimetry. Journal of Atmospheric and Oceanic Technology, 31, 1337-1362.

Dodet, G. and Piollé, J-F. (2021): Calibration of Level 2 Jason-3 GDR-F significant wave heights against in situ measurements. Technical Report (Ifremer).

Gourrion, J.; Vandemark, D.; Bailey, S.; Chapron, B.; Gommenginger, G.P.; Challenor, P.G.; Srokosz, M.A. (2002): A Two-Parameter Wind Speed Algorithm for Ku-Band Altimeters. J. Atmos. Ocean. Technol., 19, 2030–2048.Kopsinis Y. (2009): Development of EMD-based denoising methods inspired by wavelet thresholding. IEEE Transacions on Signal Processing 57(4):1351-1362. DOI: 10.1109/TSP.2009.2013885

Hanna, S. & Heinold, D. (1985). Development and application of a simple method for evaluating air quality. In: API Pub. No. 4409, Washington, D.C. Washington, U.S.A.

Mentaschi, L., Besio, G., Cassola, F., & Mazzino, A. (2013). Problems in RMSE-based wave model validations. Ocean Modelling, 72, 53-58.

Queffeulou P. (2016): Validation of Jason-3 altimeter wave height measurements (poster). OSTST meeting, November 1-4, 2016, La Rochelle, France.

Queffeulou P. and Croizé-Fillon D. (2017): Global Altimeter SWH Data Set, version 11.4, February 2017. Technical report Ifremer. (ftp://ftp.ifremer.fr/ifremer/cersat/products/swath/altimeters/waves/documentation/altimeter_wave_merge__11.4.pdf)

Quilfen Y. and Chapron B. (2019): On denoising satellite altimeter measurements for high-resolution geophysical signal analysis. Submitted to Advances in Space Research special issue “25 Years of Altimetry” Sentinel-3 Team, 2013, Sentinel-3 User Handbook v1.0.

Tran N. (2014): Updated wind speed and sea state bias models for Ka-band altimetry. Poster, OSTST 2014 available at : https://meetings.aviso.altimetry.fr/fileadmin/user_upload/tx_ausyclsseminar/files/Poster_PEACHI_ssb_tran2014.pdf

IX LIST OF ACRONYMS

AL	Saral/AltiKa
C2	Cryosat-2
CalVal	Calibration/Validation
CF	Climate Forecast (convention for NetCDF)
CFO	CFOSAT mission
CLS	Collecte Localisation Satellite
CMEMS	Copernicus Marine Environment Monitoring Service
DAD	Dynamic Acquired Data
DGF	Direct Get File (FTP-like CMEMS service tool to download a NetCDF file)
DT	Delayed Time
DU	Dissemination Unit
EUMETSAT	European Organisation for the Exploitation of Meteorological Satellites
FTP	File Transfer Protocol
GDR	Geophysical Data Record
GMSL	Global Mean Sea Level
GOP	Geophysical Ocean Product
H2B	HaiYang-2B mission
IGDR	Intermediate Geophysical Data Record
J3	Jason-3
L2/L2P/L3/L4	Level 2 / Level 2 Plus / Level 3 / Level 4
LRM	Low Resolution Mode
MOTU	Web server allowing the distribution of met/ocean gridded data files through the web (https://github.com/clstoulouse/motu)
NetCDF	Network Common Data Form
NOP	NRT Ocean Product
NRT	Near Real Time
OE	Orbit Error
OGDR	Operational Geophysical data record
PLRM	Pseudo LRM
QUID	QUality Information Document
RCP	Remote Call Procedure
RMS	Root Mean Square
RPC	Remote Protocol Client
RT	Real Time
S3A	Sentinel-3A
S3B	Sentinel-3B
S6A	Sentinel-6A
SAD	Static Acquired Data

SAR	Synthetic Aperture Radar
SARIn	SAR Interferometric
SPC	SPeCtral
Subsetter	CMEMS service tool to download a NetCDF file of a selected geographical box and time range
SWH	Significant Wave Height
SWOT	Surface Water and Ocean Topography
TAC	Thematic Assembly Center
TDS	Thredds Data Server
VAVH	Visual AVerage Height
WMS	Web Map Service